THESIS

3 1293 10062 8779

LIBRARY
Michigan State
University

This is to certify that the

thesis entitled

ORGANIZATION OF PROJECTION NEURONS IN THE RAT HYPOTHALAMIC PARAVENTRICULAR NUCLEUS

presented by

William Earl Armstrong

has been accepted towards fulfillment
of the requirements for

PH.D. degree in Psychology-Neuroscience

Glenn I. Hatton
Major professor

Date 9/5/79

O-7639

OVERDUE FINES ARE 25¢ PER DAY
PER ITEM

Return to book drop to remove
this checkout from your record.

ORGANIZATION OF PROJECTION NEURONS IN THE RAT HYPOTHALAMIC PARAVENTRICULAR NUCLEUS

By

William E. Armstrong

A DISSERTATION

Submitted to
Michigan State University
in partial fulfillment of the requirements
for the degree of

DOCTOR OF PHILOSOPHY

Department of Psychology; Neuroscience Program

1979

ABSTRACT

ORGANIZATION OF PROJECTION NEURONS IN THE RAT
HYPOTHALAMIC PARAVENTRICULAR NUCLEUS

By

William E. Armstrong

Projection neurons in the rat hypothalamic paraventricular nucleus (pv) were identified using the retrograde transport of horseradish peroxidase following injections of this tracer into the neurohypophysis, jugular vein, lower brainstem, spinal cord, amygdala and septum. The objective was to compare the distribution of neurohypophysial-projecting neurons to that of cells projecting either extrahypothalamically or to the arcuate-median eminence region of the hypothalamus. Immunohistochemical investigations allowed the additional comparison of the distribution of pv neurophysin (NP)-containing neurons to that of projection neurons in order to determine which projection neurons might be potential sources of NP-containing pathways projecting both in and outside the hypothalamus.

Beginning rostrally, it was observed that the anterior commissural nucleus (ac) contains many magnocellular perikarya which: 1) project to the neurohypophysis but apparently not to those regions outside the hypothalamus that were studied; 2) contain NP; and 3) are actually separated from the pv by 300-400 μm. Proceeding caudally,

the medial (pvm) and lateral (pvl) magnocellular pv neurons exhibit some of the same characteristics lised for ac cells, i.e., these cells project to the neurohypophysis and most often contain NP. In addition, a few scattered magnocellular neurons of the pvm and pvl were found to project to the septum and amygdala. Most small-medium sized cells in the dorsomedial cap and cells of varying sizes in the extreme posterior pv (pvpo) were not found to project to the neurohypophysis, but were observed to connect with the brainstem and/or spinal cord. Large pvpo cells and a few medium sized cells of the dorsomedial cap were shown to contain NP. A few cells of the pvpo also transported horseradish peroxidase from the septum and amygdala.

Small cells of the medial parvocellular zone were found to project to the acruate-median eminence region and to the brainstem, spinal cord, amygdala and septum. Rarely, a small cell was found to contain NP.

Although zones of overlap were noted, the results suggest that cells of the pv are segregated into neurohypophysial-projecting groups and groups projecting to other regions. The former consist of mostly pvm and pvl magnocellular neurons which contain NP, while the latter include cells of the dorsomedial cap, pvpo and medial parvocellular zone which may or may not contain NP and which range in size from small to large.

In terms of the number of identified projection neurons, those connecting with the neurohypophysis and brainstem and/or spinal cord form the most significant cell groups of the pv. The distribution of these cells corresponds with regional cell clustering in the pv as observed in Nissl-stained material. The topographic separation

and morphological differentiation of putative pv subnuclei which maintain separate efferent connections suggest that the cells of these subdivisions may function independently.

ACKNOWLEDGEMENTS

I give many thanks to Dr. Glenn I. Hatton for his enthusiastic support of this project and for his continual creative input which has guided my graduate career. I also thank the members of my committee, Drs. Charles D. Tweedle, Stephen T. Kitai and John I. Johnson, for offering helpful suggestions.

I am extremely grateful for the technical service I received during this project, provided by Jeff Burstyn, Al Doran, Jim Hatton, Ron Ragotsky and Cathy Young. Dr. Tom McNeill of the University of Rochester, Department of Anatomy, provided immunohistochemical data which formed a substantial part of the dissertation and which added immeasurably to the significance of the results.

The pertinent advice and contributions of Steven Warach during the preparation of a portion of this dissertation were invaluable. Also, due largely to his knowledge of the literature and unique points of view, the comments of William Gregory on an earlier version of a portion of the dissertation were very much appreciated.

TABLE OF CONTENTS

LIST OF FIGURES

LIST OF ABBREVIATIONS

ac	anterior commissural nucleus
acc	accessory neurosecretory nuclei
aco	anterior commissure
ah	anterior hypothalamic area
ar	arcuate nucleus
bla	basolateral nucleus of the amygdala
bmea	basomedial nucleus of the amygdala
bnst	bed nucleus of the stria terminalis
cc	corpus callosum
cd-p	caudate-putamen
cea	central nucleus of the amygdala
coa	cortical nucleus of the amygdala
cp	cerebral peduncle
dm	dorsomedial hypothalamic nucleus
ed	endopiriform nucleus
fx	fornix
hnt	hypothalamo-neurohypophysial tract
hpc	hippocampus
ic	internal capsule
l	lateral
la	lateral nucleus of the amygdala
lpo	lateral preoptic area
ls	lateral septal nucleus
lv	lateral ventricle
m	medial
me	median eminence
MEex	external layer of the median eminence
mea	medial nucleus of the amygdala
mpo	medial preoptic area
ms	medial septal nucleus
nc	nucleus circularis
ncor	neocortex
ndb	nucleus of the diagonal band of Broca
oc	optic chiasm
ot	optic tract
pem	magnocellular periventricular cells
pv	paraventricular nucleus
pvdc	dorsomedial cap of the paraventricular nucleus
pvl	lateral magnocellular paraventricular nucleus
pvm	medial magnocellular paraventricular nucleus
pvpa	parvocellular portion of the paraventricular nucleus
pvpo	posterior portion of the paraventricular nucleus

rs	rhinal sulcus
sc	suprachiasmatic nucleus
sg	substantia gelatinosa
sm	stria medullaris
sptr	spinal trigeminal nucleus
soa	anterior portion of the supraoptic nucleus
sot	tuberal portion of the supraoptic nucleus
st	stria terminalis
th	thalamus
thpva	thalamic paraventricular nucleus, anterior portion
v	third ventricle
vm	ventromedial hypothalamic nucleus
zi	zona incerta

INTRODUCTION

Background

Since the seminal investigations of Wolfgang Bargmann and Ernst and Berta Scharrer (e.g., Bargmann and Scharrer, 1951; see Bargmann, 1966, for review), the mammalian hypothalamic paraventricular and supraoptic nuclei have been considered neurosecretory structures. Magnocellular neurons of these nuclei synthesize the nonapeptide hormones oxytocin (OX) and vasopressin (VP) as well as the associated "carrier" proteins of these substances, neurophysin (NP) I and II, respectively (see Defendini and Zimmerman, 1978, for review).

Once thought to terminate solely within the neurohypophysis for hormone release into the general circulation via neurohemal contacts, axons issuing from the paraventricular nucleus (pv) are now thought to innervate many sites within the central nervous system. Although the terminal portions of these projections have yet to be systemically examined, in some cases conventional synapses may be formed by putative peptidergic axons (Sterba, Hoheisel, Wegelin, Naumann and Schober, 1979).

In the rat, those areas most frequently cited to receive pv projections include the brainstem and spinal cord (Buijs, 1978; Conrad and Pfaff, 1976; Hancock, 1976; Hosoya and Matsushita, 1979; Ono, Nishino, Sasaka, Muramoto, Yano and Simpson, 1978; Saper, Loewy, Swanson and Cowan, 1976; Swanson, 1977), amygdala (Buijs, 1978;

Conrad and Pfaff, 1976; Sofroniew and Weindl, 1978a), septum (Conrad and Pfaff, 1976) and the external layer of the median eminence (MEex) (Vandesande, Dierickx and De Mey, 1977). It is uncertain whether the same cells which project to the neurohypophysis also send axons to these areas.

In their early investigations of hypothalamic cytoarchitecture, Gurjdian (1927) and Krieg (1932) proposed a simple division of the rat pv into lateral magnocellular and medial parvocellular groups. These divisions may account for two major cell clusters, but recent data have shown that pv magnocellular neurons are not a functionally (e.g., Poulain, Wakerley and Dyball, 1976; Richard, Freund-Mercier and Moos, 1978) nor a morphologically (Barry, 1975; Defendini and Zimmerman, 1978; Hancock, 1976; Hatton, Hutton, Hoblitzell and Armstrong, 1976) homogeneous group. Cells in the anteroventromedial (pvm) portion are smaller and less often contain multiple nucleoli than do cells in the posterodorsolateral (pvl) division (Hatton et al., 1976). Being more anterior, the pvm probably contains more OX-producing neurons than does the pvl, while the latter more likely includes a comparatively greater proportion of VP-producing cells (Choy and Watkins, 1977; Defendini and Zimmerman, 1978; Swaab, Pool and Nijveldt, 1975). A further clumping of OX cells laterally and VP neurons medially has also been described (Defendini and Zimmerman, 1978; Vandesande and Dierickx, 1975).

One might expect the observed heterogeneity in the distribution of OX- and VP-containing cells within the pv to be related to the distribution of pv projection neurons. For example, the concentration of OX within the medulla oblongata is ten times that of VP. In the septum the levels are similar, and in the amygdala significant amounts

of VP, but not OX, can be detected (Dogterom, Snijdewint and Buijs, 1978). Additionally, immunocytochemical studies indicate that more VP- than OX-positive fibers are present in the rostral portions of the brain (e.g., hippocampus, amygdala), whereas OX fibers are more densely distributed caudally (Buijs, 1978).

Statement of problem

The problem remains that despite extensive documentation of pv projections to targets other than the neurohypophysis, the location of the cells giving rise to these pathways has yet to be compared with: 1) the distribution of pv cells projecting to the neurohypophysis; 2) the distribution of pv hormone-containing neurons; and 3) pv cytoarchitecture.

In a preliminary investigation it was determined that horseradish peroxidase (HRP) injected into the neurohypophysis was retrogradely transported by cells of the pvm and pvl, but in other portions of the nucleus, notably the extreme posterior component (pvpo), labelling was virtually absent (Armstrong and Hatton, unpublished observations). More recently, it has been documented that the morphology of pvm, pvl and pvpo cells differs as seen in Golgi-like profiles (Armstrong, Warach, Hatton and McNeill, 1979). Thus, it is suggested that the pv may be characterized by subnuclei.

The present investigation's major aim was to determine if pv neurons projecting to the lower brainstem, spinal cord, septum, amygdala and MEex have a similar or different distribution than cells projecting to the neurohypophysis, using HRP histochemistry. These areas were chosen since they are most often cited to receive pv fibers, as shown with autoradiography of anterogradely transported proteins, immunohistochemistry of pv intrinsic hormones and the

retrograde transport of HRP. In addition, the immunocytochemical detection of NP was used to localize hormone-containing cells, allowing a comparison of these to the location of projection neurons.

In this investigation particular attention was paid to the regional subdivisions of the pv apparent in Nissl-stained material. This was done to determine the relationship among subnuclei, projection neurons and NP-containing cells. Included for study was Peterson's (1966) anterior commissural nucleus (ac), since some investigators apparently consider this structure to be an extension of the pv (see Figure 4A in Buijs, Swaab, Dogterom and Van Leeuwen, 1978; and Figure 14 in Christ, 1969).

MATERIALS AND METHODS

Animals and surgical procedures

All animals used in this study were male albino rats purchased from the Holtzman Company. Their ages ranged from 40-60 (vascular HRP injections) and 60-120 (all other injections and NP staining) days. Housing was provided in wire mesh cages which were kept in a constantly illuminated room. Food (Wayne Mouse Breeder Blox) and tap water were available at all times.

In experiments requiring surgery, the rats were anesthetized with sodium pentobarbital (50 mg/kg, intraperitoneally). Ether was often used as a supplemental anesthetic, and was used exclusively for perfusions.

Normal material

Brains embedded in celloidin or paraffin and sectioned in one of the three standard planes at 22 or 6 μm, respectively, were available for examination from previous studies (Armstrong and Hatton, 1978; Hatton and Walters, 1973; Hatton et al., 1976). In all cases at least one set of alternate sections was stained with thionine to demonstrate Nissl material; in some cases the remaining set was stained with the Weil or Sanides Heidenhain method for the demonstration of myelinated fibers.

HRP injections and processing

For all of the preparations except blood injections, relatively large (0.15-1 µl) amounts of 30% HRP (Sigma VI or Miles) in 0.89% saline were delivered intraparenchymally via pressure. In most cases 2% dimethyl-sulfoxide (Keefer, 1978) or 0.5% poly-L-ornithine (Itaya, Williams and Engel, 1978; Hadley and Trachtenberg, 1978) were added to the HRP solution in order to increase the amount of uptake. In some cases both were added to the HRP solution.

The purpose in making large injections was an attempt to label as many pv neurons as possible which might project to a given structure, the only limitation being to avoid spread to other structures under study. Thus, to define terminal locations was not a primary goal.

Neurohypophysial injections. Successful pressure injections aimed toward the neurohypophysis were made via both dorsal (n=4) and intra-aural (n=5) approaches. Several more animals in which an inadequate amount of HRP was delivered, or the injection misplaced, served as controls. With both approaches a 5 µl syringe (Hamilton) equipped with a 31 ga needle was used to deliver from 0.15 to 1 µl of HRP solution.

For the dorsal approach, the coordinates were 3-3.5 mm anterior to ear bar zero with the animal's skull horizontally positioned. The syringe was mounted onto a Kopf stereotaxic apparatus with a Kopf syringe holder and the needle was lowered to the bottom of the skull, then raised 0.5-1 mm. A microdrive attached to the stem of the holder was used to manually deliver the solution over a period

of 1-30 min. The same syringe and apparatus were used to make brainstem, spinal cord, amygdalar and septal injections.

The pituitary was approached intra-aurally with the aid of Kopf hypophysectomy ear bars. Coordinates were first determined from dead rats, the brains of which had been removed to reveal the pituitary. In rats of a similar size a 20 ga needle serving as a guide cannula was inserted through the ear canal and bulla, and the 31 ga needle of a 5 µl syringe containing the HRP solution was then placed through the cannula to the midline. Rats receiving neurohypophysial injections were allowed to survive from 12-48 hr.

Brainstem and spinal cord injections. The lower medulla oblongata and spinal cord were approached dorsally. In four rats multiple (1-5) unilateral injections were made in the vicinity of the nucleus of the solitary tract, dorsal motor nucleus of the vagus nerve and surrounding structures with either a micropipette (30-50 µm tip, outside diameter) attached to a 1 µl syringe or with a 31 ga needle affixed to a 5 µl syringe. From the obex, the coordinates used were: anterior-posterior, from 0.0-1 mm anteriorly; medio-lateral, from 0.5-1 mm laterally; dorso-ventral, from 0.5-2 mm ventral to the brain surface. Two rats received an injection either between levels C1 and C2, or T3 and T4 of the spinal cord after a hemisection of the same side at the injection site (see Results for placements). A seventh control rat received a 1 µl injection into the fourth ventricle above the obex.

Amygdalar injections. Twelve rats received successful injections into the amygdala. The amygdala was approached laterally following removal of the parieto-temporal bone and zygomatic arch. Using a

31 ga needle of a 5 µl syringe, preparations ranged from a single 0.1 µl placement to multiple (8) injections totalling 1.55 µl. Coordinates used were: anterior-posterior, from 2.3-2.9 mm posterior to the coronal suture; dorso-ventral, from 1 mm above to 1 mm below the rhinal sulcus; medio-lateral, from 1-4.5 mm below the brain surface. The needle was situated at an angle 20-40° to the horizontal plane. Survival times ranged from 24-48 hr, with most animals being sacrificed after 36 hr.

Septal injections. The septum was approached dorsally and the HRP was successfully deposited in eight rats using a 31 ga needle as described previously. Coordinates used were: anterior-posterior, from 0.3 mm anterior to 1.5 mm posterior to the coronal suture; medio-lateral, from 0.5-1 mm lateral to the sagittal suture; dorso-ventral, from 5-5.6 mm below the skull surface. For medial injections the needle was placed at an angle 5° to the vertical plane, thus avoiding penetration of the sagittal sinus. Only single penetrations with injections of 0.15-0.2 µl were made. Survival times ranged from 20-36 hr.

Vascular injections. Intrajugular injections of HRP were made to: 1) insure that pv cell labelling from neurohypophysial injections was not due to spread of the enzyme through the vasculature; and 2) determine if cells additional to those labelled by neurohypophysial injections could be marked. Additional labelling might then indicate an innervation of the MEex or perhaps another neurohemal organ by the pv.

Eleven animals received successful injections of 0.5 ml 10% HRP (Sigma) dissolved in sterile saline into the jugular vein. Following

exposure of the vein and overlying muscle, a 24 or 26 ga needle attached to a tuberculin syringe (1 cc) was inserted through the muscle into the vein. Injection times ranged from 30-60 sec, after which the animals were allowed to survive 1/2 (n=2), 6 (n=2), 12 (n=2), 24 (n=2) or 48 (n=3) hr. Neither dimethylsulfoxide nor poly-L-ornithine were added to the HRP in these experiments.

Histology. Rats receiving HRP injections were perfused with 0.89% saline followed by a solution of 1% paraformaldehyde, 1.25% glutaraldehyde in 0.1 M phosphate buffer (pH = 7.2-7.4). Further perfusion was often carried out with a cold solution of 10% sucrose buffer. In other cases, however, the brain was removed after the initial perfusion and fixed an additional 24 hr at 4°C prior to transfer to a cold 30% sucrose buffer solution. For those rats receiving the sucrose buffer perfusion, the brains were removed from the skulls and placed in the same sucrose buffer solution for 24 hr before sectioning.

Coronal sections were taken at 30 or 60 μm and collected in cold 10% sucrose buffer, where they were kept for up to 48 hr prior to reacting with one of several different chromogens, including 3-3' diaminobenzidine (DAB), Hanker-Yates reagent (H-Y), benzidine dihydrochloride (BDHC) or tetramethylbenzidine (TMB). In all cases one set of alternate sections was reacted with either BDHC or TMB; the remaining set was reacted with either DAB or H-Y, both with and without cobalt intensification (Adams, 1976). Procedures for use of BDHC and TMB were followed according to Mesulam (1976, 1978); for DAB and H-Y the methods of Nauta, Pritz and Lasek (1974) and Hanker, Yates, Metz and Rustioni (1977), respectively, were employed. Sections were

counterstained with Neutral red or Safranin-O when BDHC or TMB was used, and with thionine when DAB or H-Y was used. The tissue was examined with both bright and darkfield condensors. Positive cells were plotted in some cases with the aid of a deflecting prism (Zeiss) and drawing tube, or by using a low power micro-projecting device (Ken-A-Vision). In some instances cell counts were made using a Whipple-Hauser reticule under 312.5x power.

Neurophysin (NP) staining

Two rats were perfused with Bouin's fixative following a 0.89% saline rinse. The brains were removed, post-fixed from three to four days, dehydrated in alcohol, cleared in methyl benzoate and embedded in paraffin. Two of every eight 10 μm sections were mounted from warm water (55°C) and dried. Immunocytochemical staining for NP followed the immunoperoxidase-antiperoxidase techniques of Sternberger (1974).[1] Deparaffinized sections were rehydrated in 0.01 M phosphate-buffered saline (pH = 7.1). Rabbit antisera to bovine NP I or rat NP were provided by Dr. A. G. Robinson. Bovine NP I antiserum was incubated at a dilution of 1:1000 for 24 hr at 4°C while rat NP antiserum was used at 1:3000 for the same length of time. In control sections phosphate-buffered saline was substituted for the primary antisera in the immunoperoxidase bridge. Some sections were lightly counterstained with cresyl violet following the immunohistochemical procedures.

Antisera to bovine NP I and rat NP previously have been characterized by radioimmunoassay (Robinson, Zimmerman, Engleman and Frantz, 1971; Seif, Huellmantel, Platia, Haluszczak and Robinson,

---

[1]Thanks are due Dr. Tom McNeill of the University of Rochester for immunocytochemistry.

1971) and immunoabsorption controls have been reported previously at both the light (Zimmerman, Hsu, Robinson, Carmel, Frantz and Tannenbaum, 1973) and electron (Silverman and Zimmerman, 1975) microscopic levels. In addition, bovine NP I has been shown to cross-react with all rat NP and has been used for immunocytochemical (Zimmerman, Defendini, Sokol and Robinson, 1975) and radioimmunoassay (Cheng and Friesen, 1971) investigations.

RESULTS

The most important single result of this study is the finding that neurohypophysial-projecting pv neurons appear to be relatively segregated from those projecting to the brainstem, spinal cord, septum and amygdala. Since the distribution of projection neurons reveals a pv which is structurally more complex than earlier observers (e.g., Bodian and Maren, 1951; Gurdjian, 1927; Kreig, 1932) had considered, a reexamination of its cytoarchitecture in Nissl-stained sections seems warranted. This description should aid the reader in appreciating the location of neurons labelled by the techniques used in this study. Furthermore, it supports the notion that individual cell morphology and patterns of cell clustering are related to the metabolic capacities and anatomical connections of neurons.

Reference throughout this dissertation will be made to parvocellular (small), magnocellular (large) and medium sized neurons. In general, small cells are defined as those with long somal diameters measuring less than 14 μm. Medium sized cells range from 14-17 μm along this dimension, and large cells are those with a long diameter which is greater than 17 μm. Few cells in any of the areas discussed were greater than 25 μm across the long axis. While precise cell measurements were not made, using the reticule a cell could be placed in one of these categories and its size estimated.

Observations of Nissl-stained material

Anterior commissural nucleus (ac). The ac is best viewed in the coronal plane, where it first appears as a distinct clump of darkly staining cells lying below and slightly medial to the descending column of the fornix in the dorsal preoptic area, just posterior to the midline portion of the anterior commissure (Figure 1A). Proceeding caudally, this loosely packed group of cells takes a position more medial to the fornix and close to the third ventricle (3 V), being separated from the latter by scattered small cells, glia and a line of vertically oriented, darkly staining, magnocellular neurons which often abut the ependyma (Figure 1B). The suprachiasmatic nucleus, preoptic portion of the bed nucleus of the stria terminalis, anterior supraoptic nucleus and medial preoptic area can all be found in the same coronal plane through the ac, thus aiding in distinguishing the latter from the anterior part of the pv. The ac begins at about the same level as the suprachiasmatic nucleus and extends rostracaudally for about one-half the length of the latter structure. A scatter of magnocellular periventricular neurons at the dorsolateral edge of the 3 V extends to nearly the rostal limit of the pv.

Cells of the ac are normally not quite as large as the magnocellular neurons of the pv, with their long somatic axes only rarely reaching 20 μm in celloidin- or paraffin-embedded material (Figure 3A). Except for their slightly smaller size, the rounded cells of the ac are similar to most other magnocellular neurosecretory cells, containing one or sometimes two prominent nucleoli, a dense rim of Nissl substance, and a large round or oval nucleus which is seldom invaginated (Figure 3A). Most of the ac cells have their long axes in the

Figure 1. Photomicrographs of thionine-stained, celloidin-embedded, coronal sections through the major divisions of the ac and pv with surrounding hypothalamus. Each section is 22 μm in thickness. The number of similar sections *between* those shown varies as follows: A-B: 7; B-C: 11; D-E: 3; E-F: 5; F-G: 7; G-H: 5. See text for description.

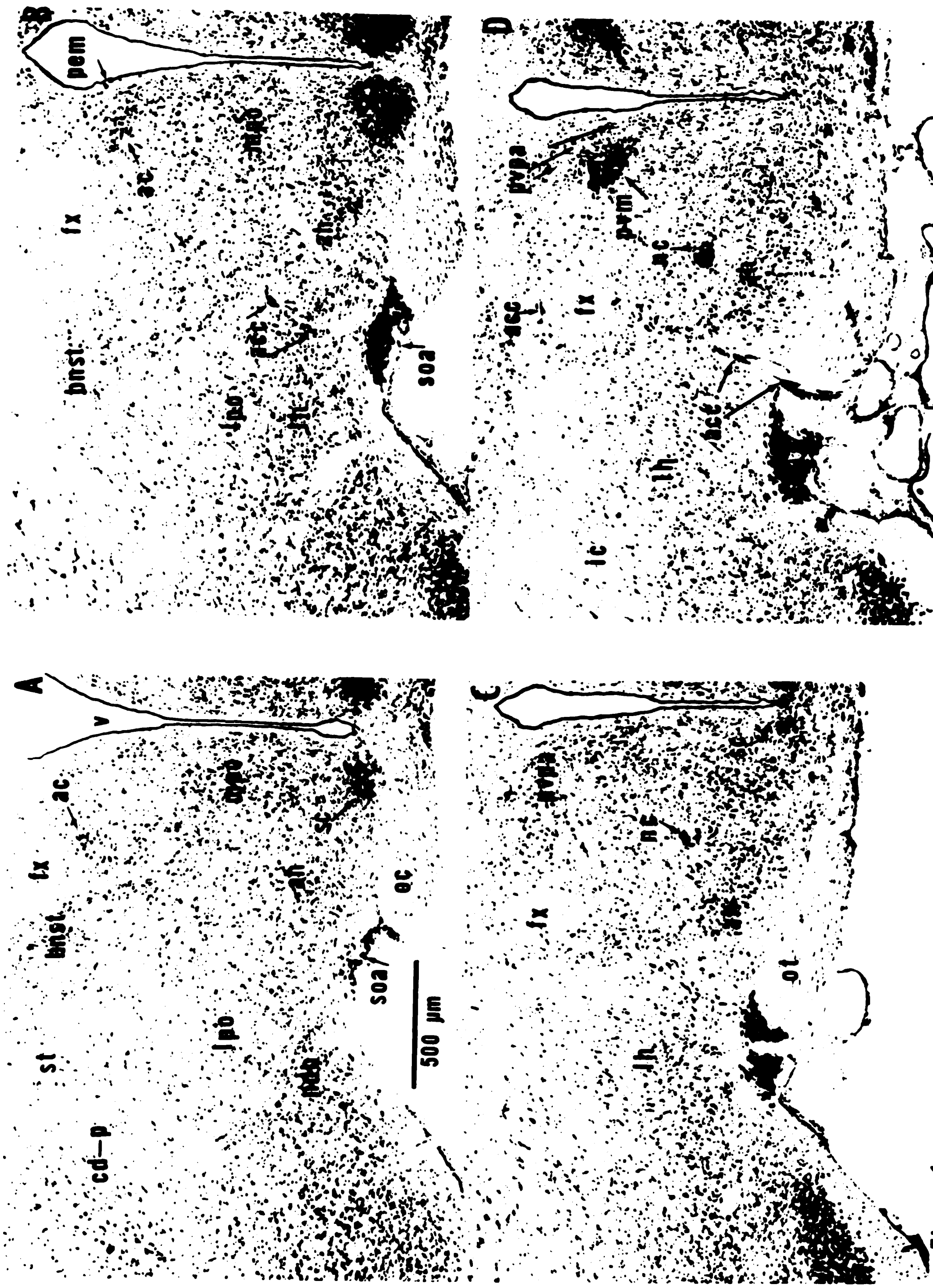

Figure 1

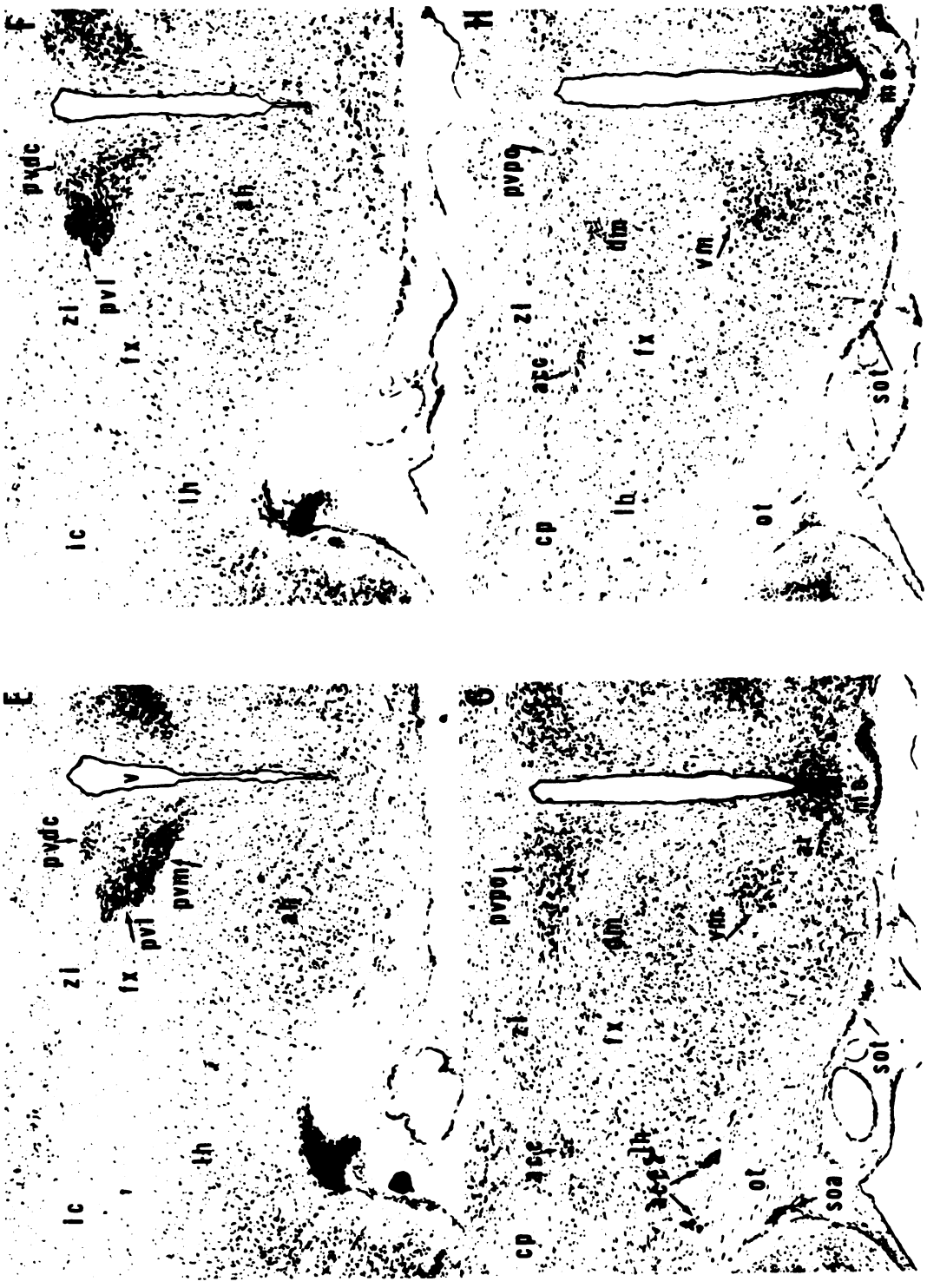
F
pvdc
zi
pvi
fx
lc
lh
H
pvpo
zi
dm
vm
fx
cp
lh
ot
sol
E
pvdc
v
zi
pvi
pvm
fx
lc
lh
G
pvpo
zi
dm
vtn
fx
cp
lh
ot
soa
sol

Figure 1

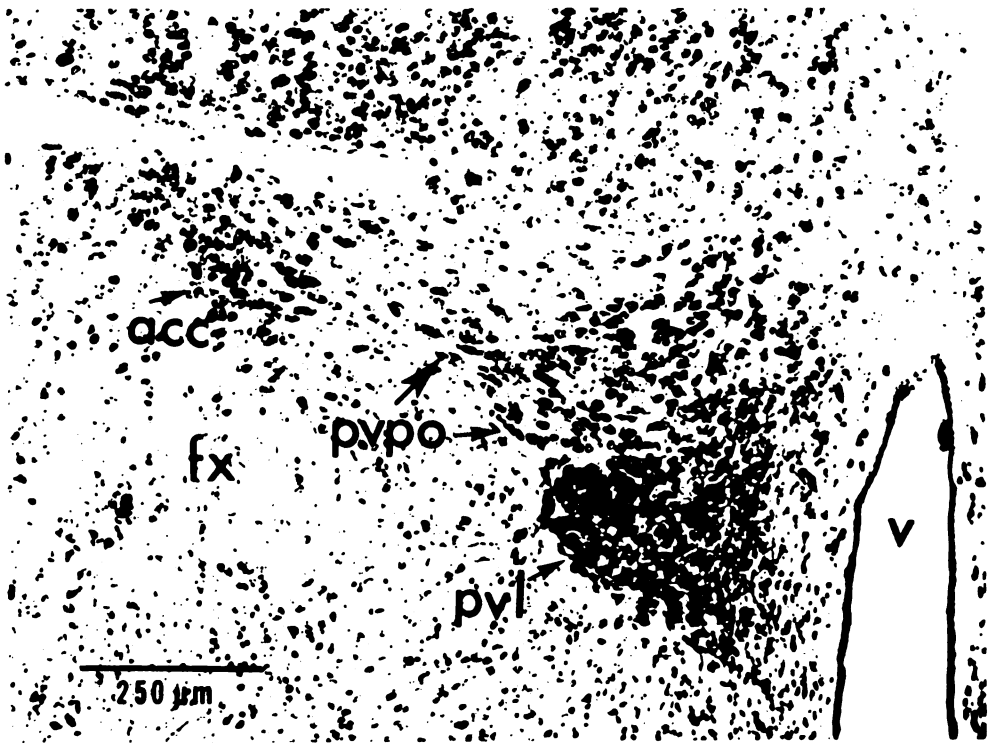

Figure 2. Photomicrograph of a 22 µm, thionine-stained, celloidin-embedded, horizontal section through the pv showing the relation of the pvpo to the pvl. Note also that the accessory group (acc) appears to be a lateral extension of the pvpo.

Figure 3. Photomicrographs of 6 μm, thionine-stained, paraffin-embedded sections showing major cell types in the ac and pv. Magnocellular ac, pvm and pvl neurons are shown in A, B and C, respectively; arrows point to cells with multiple nucleoli. (D) Parvocellular neurons near the medial edge of the pvl. Note the basophilic "stripes" in these cells (small arrows); large arrows point to two adjacent magnocellular pvl neurons for comparison. (E) Neurons of the dorsomedial cap. Arrows point to basophilic "stripes", which are also characteristic of many of these cells. (F) Neurons of the pvpo. Note the range in cell sizes. Large arrows point to magnocellular neurons; small arrows point to basophilic "stripes" in smaller cells. Note also the elongated somata of the large cells in particular.

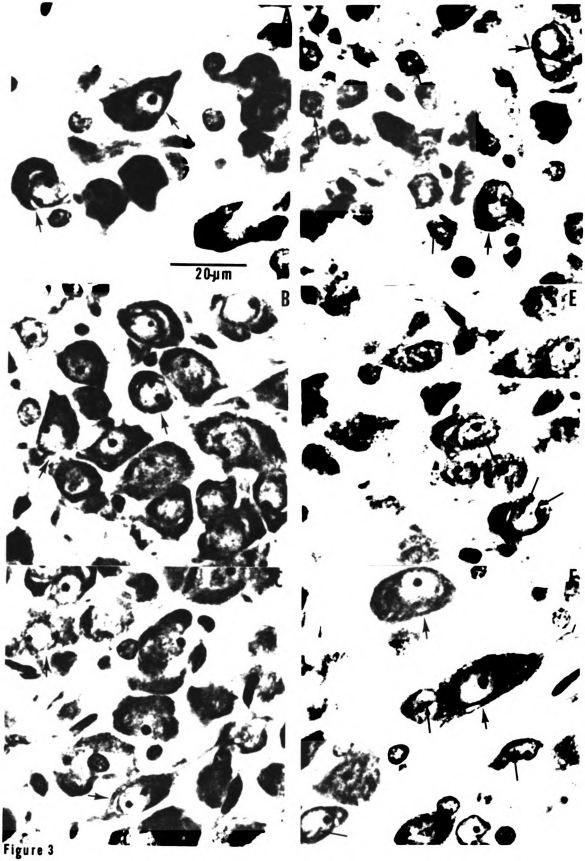

Figure 3

mediolateral plane, but exceptions are frequently encountered, these latter cells most often being situated vertically. At all levels, parvocellular cells can be found among the large neurons of the ac.

Medial magnocellular paraventricular nucleus (pvm). As with the ac, the pvm is seen to best advantage in coronal sections. Proceeding caudally and slightly ventrally from the ac, pvm cells are grouped in a band lying approximately at a 45° angle to the 3 V wall (Figure 1D). On its ventrolateral edge a cell sparse zone separates the pvm from the caudal aspect of the medial preoptic area and anterior hypothalamus. An examination of myelin-stained material failed to reveal processes in the zone. Whereas the fornix is clearly adjacent to the ac, it is quite distant from and lies dorsolateral to the pvm. At more caudal levels the pvm spreads laterally and slightly dorsally, forming a transition zone with the dense ball of cells constituting the pvl (Figure 1E). Cells of the pvm appear more oval in shape in addition to being slightly larger (∿20 μm) than cells of the ac (Figure 3B).

Lateral magnocellular paraventricular nucleus (pvl). The pvl extends laterally toward the fornix, and its posterior aspect appears in the same plane as the rostral limit of the dorsomedial hypothalamic nucleus, which borders the pvl ventrolaterally. As with the pvm, the lateral and ventral edges of the pvl are separated from the adjacent hypothalamus by a relatively cell free, myelin free zone (Figure 1E, F). At its dorsomedial edge the pvl lies contiguous with a group of slightly smaller cells (Figure 1E, F). These latter neurons of the dorsomedial cap, as I shall refer to it, are discussed below. At its extreme caudal limit, the pvl is bounded ventromedially by cells of various sizes, most of which have long axes that are slanted at a

45-60° angle toward the 3 V and follow the contour of the pv (Figure 1F). This group of cells forms the rostral extent of the extreme posterior subnucleus of the pv (pvpo) (Figure 1G), which Bodian and Maren (1951) named "nucleus magnocellularis parvocellularis" (see their Figure 12).

A previous investigation (Hatton et al., 1976) determined that the cells of the pvl are measuably larger (mostly between 20-25 μm) in all planes and in the normal state will more often contain multiple nucleoli than cells of the pvm in male rats. Some pvl cells are spindle-shaped in coronal section, with others more rounded in appearance (Figure 3C).

Posterior paraventricular nucleus (pvpo). In coronal and horizontal sections the pvpo has a triangular shape (Figures 2 and 1G). Caudally its apex extends dorsolaterally to the level of the medial edge of the fornix and is formed by elongated cells strung out in a group which, dorsally, blends with the zona incerta (Figure 1G). At all rostrocaudal levels the pvpo is bordered ventromedially by the dorsomedial hypothalamic nucleus. At the extreme posterior limit of the pvpo the apex is restricted in extent and is situated dorsolateral to the top of the 3 V, with vertically oriented small cells largely constituting the medial portion of this subnucleus (Figure 1H). At the level of the rostral parts of the arcuate and ventromedial hypothalamic nuclei the pvpo is replaced by a loosely arranged group of cells comprising Christ's (1969) dorsal hypothalamic area. The pvpo is best distinguished from the remainder of the pv in horizontal sections, where a clear difference in packing density and cell

orientation is apparent between the cells of this subdivision and those of the more rostral pvl (Figure 2).

Large neurons of pvpo stained less intensely in this material than did other pv magnocellular elements. The neurons of the pvpo vary widely in size, from large to small (Figure 3F). Nuclei with multiple nucleoli are not as prevalent in pvpo cells as they are in the cells of the pvm or pvl, and often the nuclear membrane appears indented with a basophilic "stripe" (Figure 3F). Nuclei of this type are rare in the large neurons of the pvm and pvl (Figure 3B, C). Large somata of the pvpo are measurably more fusiform than those of the other magnocellular subdivisions (Armstrong et al., 1979) and they are most often oriented mediolaterally.

Parvocellular neurons. Parvocellular pv neurons form the initial part of the pv anteriorly, lying just rostral to the pvm (Figure 1B). Parvocellular elements occupy a primarily medial position throughout the pv, but they are by no means restricted to this zone. In Nissl-stained material small cells are seen as a broadly distributed group, contain a scant amount of cytoplasm (large nucleus to cytoplasm ratio) and have a small somal diameter as opposed to the large, more cytoplasmic magnocellular neurons (Figure 3D). Small cells are contiguous with the magnocellular population at all levels of the pv, but their density is greatest dorsomedial to the pvm (Figure 1D). Small neurons can be found among the large cells of the pvl, pvm and, most notably, the pvpo. Additional clusters of small-medium sized cells occur ventromedial to the caudal portion of the pvl and in the adjacent region of the pvpo. Due to their size, the nuclear characteristics of most parvocellular elements are difficult

to determine. Often the nucleus exhibits a basophilic indentation similar to that described for some pvpo neurons (Figure 3D). The nucleoplasm is granulated and occasionally more than one nucleolus-like structure is present. Clear cases of nuclei containing multiple nucleoli are much harder to document at the light microscopic level compared with their relative frequency and unequivocal identification in magnocellular neurons.

A conspicuous group of small-medium sized cells forms the dorsomedial cap, referred to earlier. This cap appears as a bulge along the dorsal surface of pv beginning near the pvm and is most noticeable near the pvl (Figure 1E, F). It extends to and becomes continuous with the dorsomedial aspect of the pvpo. Most of the cells in the dorsomedial cap are medium in size and usually possess a single prominent nucleolus in an oval nucleus. The nucleus may often be distinguished by a basophilic "stripe" (Figure 3E). In this regard the cells of the dorsomedial cap are similar to the parvocellular population in general and to many neurons of varying sizes in the pvpo.

HRP injections

Mesulam's (1978) TMB protocol proved to be the most sensitive of those tried in localizing HRP, as judged by the relatively large number of labelled cells and the readily observable anterogradely transported HRP obtained with this method. However, the poor counterstaining afforded by the red stains made alternate sections counterstained with thionine invaluable for determining the relative positions of labelled cells. Furthermore, the dense core at the center of the injection site was more easily identified using either H-Y or DAB, since reacted TMB appears more diffuse and homogeneous than these chromogens.

By far the largest number of labelled pv neurons resulted from neurohypophysial, vascular and brainstem/spinal cord injections compared to septal and amygdalar injections. In particular, the parcelling of neurohypophysial- and brainstem/spinal cord-projecting neurons into distinct subnuclei, in my opinion, characterizes much of the cytoarchitectural organization of the pv. As such, the results of these experiments are considered first and are displayed in Figures 4 through 8, where they are compared with the results of NP staining. The results of vascular, amygdalar and septal injections are then considered and may be compared with these results. For continuity, the results of the NP-localization are given after considering all of the HRP data.

Neurohypophysial afferents: anterior commissural nucleus (ac). Typically, cells of the ac were more lightly labelled than those of the pv or supraoptic nucleus following HRP injections into the neurohypophysis and in this regard these cells were similar to those of other accessory magnocellular nuclei (Peterson, 1966; Sherlock, Field and Raisman, 1975). In one animal which received a small (0.15 µl) injection and survived for 48 hr, the ac and several other accessory cells contained no labelled cells. In all other rats the ac was clearly labelled (Figure 4C). HRP-positive somata were seen rostrally beneath the fornix and at more caudal levels could be found near the 3 V, just lateral to the extensive band of magnocellular periventricular neurons which were also heavily labelled (Figures 4C; 8II A). A few large ac cells did not transport HRP in these animals as well. The size of labelled ac cells is generally smaller than that of most labelled pv neurons. In densely filled cells, medially directed

processes were commonly observed. A clear termination of HRP-labelled ac cells was evident 300-400 μm rostral to the first labelled neurons of the pv, which were located in the pvm.

Neurohypophysial afferents: paraventricular nucleus (pv). Regardless of the injected volume or approach, the distribution of HRP-labelled neurons within the pv was similar in four rats in which it was determined that spread of the enzyme was effectively confined to the neurohypophysis. This distribution is illustrated in Figures 8 II and 5-7C, prepared from sections of rat 061178. This animal received 0.15 μl of HRP via the intra-aural approach and survived 48 hr post-injection. Cells of the pvm, pvl and pv accessory neurons above the fornix were heavily marked (Figures 5 and 6C; 8 IIB, C and D), but many large labelled cells were found scattered among the medial parvocellular neurons. Uptake was conspicuously absent in the great majority of small neurons and sparse in cells of the dorsomedial cap and pvpo (Figures 4-7C). A few large cells immediately medial to the pvl were consistently unlabelled. It is noteworthy that virtually all magnocellular supraoptic cells were labelled by these injections, indicating that the heterogeneity in pv labelling was probably not due to the differential access of terminals in the neurohypophysis to the HRP.

Although the dense cell packing in the pvm and pvl prevents an assessment of the morphological details of the component neurons, it was evident that reactive processes emerge from only the lateral and medial aspects of these subnuclei. In one rat receiving a large (1 μl) injection, fine labelled processes were seen emanating from the lateral aspects of the pvm and pvl, forming the paraventricular

Figures 4-7. Photomicrographs of the ac and pv in coronal section. In each figure, A is from a 22 μm thionine stained, celloidin-embedded section, providing reference to the location of the structure under consideration; B is from a 10 μm paraffin-embedded section stained for NP (rat antiserum); C and D are darkfield photomicrographs of 60 μm frozen sections stained for HRP (TMB protocol) after injections into the neurohypophysis (C) or brainstem (D). Figure 4, ac; 5, pvm; 6, pvl; 7, pvpo. Rat 01177 (1 μl into the neurohypophysis, 48 hr survival) is represented in Figure 4C; all other sections from neurohypophysial injections are from rat 061178 (0.15 μl, 48 hr survival). Rat 34179 (0.5 μl into brainstem, 48 hr survival) is represented in part D of all figures. In Figure 4B, arrows point to magnocellular periventricular neurons. In Figure 4C, small white arrowheads point to magnocellular periventricular neurons. In Figure 6D, large arrow points to ventromedial, labelled neurons which lie just caudal to the pvm and form the rostral extension of the pvpo. Note the relative segregation of neurons projecting to the brainstem from those projecting to the neurohypophysis. Note also that cells in both groups of neurons may contain NP. In Figure 6D anterogradely transported HRP reveals the extent of the pvl. Anterograde transport of HRP to hypothalamus was not observed after spinal cord injections. For scale, see Figure 4A.

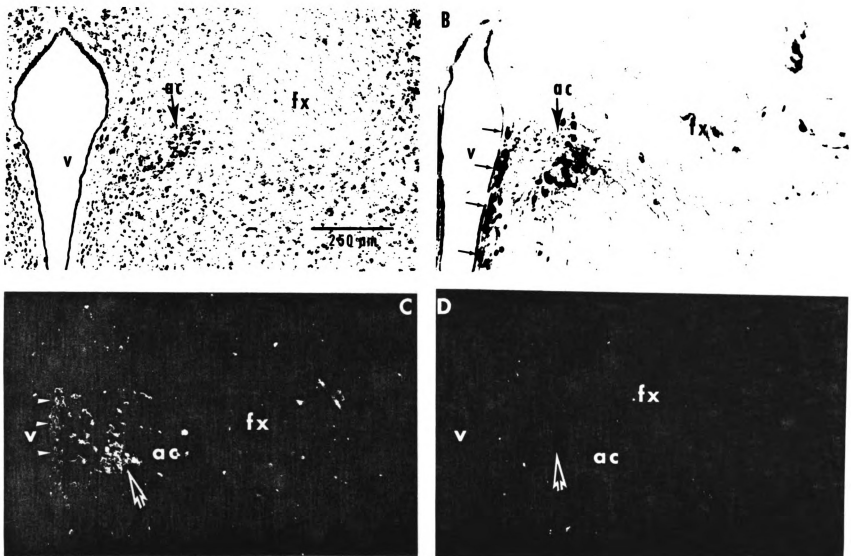

Figure 4

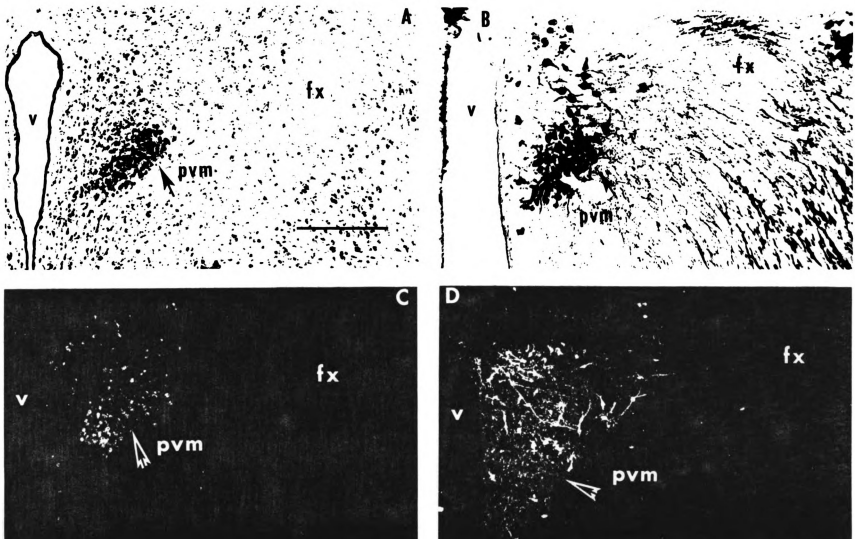

Figure 5

Figure 6

Figure 7

Figure 8. Diagram from tracings of coronal sections through the hypothalamus depicting the distribution of NP (I; rat antiserum), HRP-labelled cells following a neurohypophysial injection (II; rat 061178) and HRP-labelled cells ipsilateral to a brainstem injection (III; rat 34179). Within a row (A-I) tracings are taken through approximately the same portion of the ac or pv for each treatment (columns I-III). Small dots represent positive cells. Large blackened areas represent filling of virtually all cells within the area. Fine lines represent NP-positive fibers in I. In IIIA, the outline of the ac has been drawn in. In IIIB, the outline of the pvm has been drawn in, and in IIIC and D the outline of the pvl has been drawn in. For clarity, only the tracings in column II have been labelled, except for fibers which are revealed by the NP stain, which are labelled in I. Note the correlative distribution of NP-positive and HRP-labelled perikarya. Note in I the differences in the initial fiber trajectories emanating from the ac, pvm, pvl and pvpo.

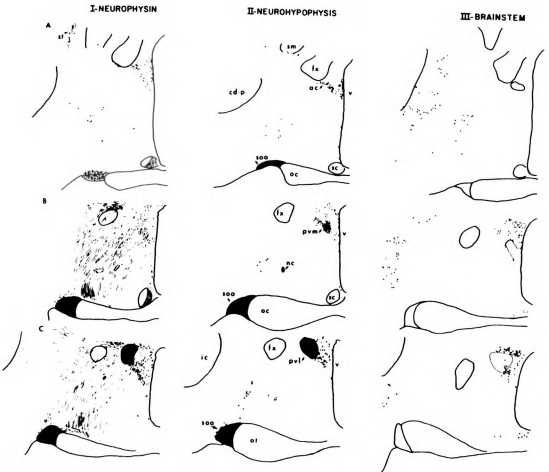
I-NEUROPHYSIN
II-NEUROHYPOPHYSIS
III-BRAINSTEM
A
B
C
st
cdp
sm
ls
acc
v
soo
oc
ic
pvma
pc
pvl
ot

Figure 8

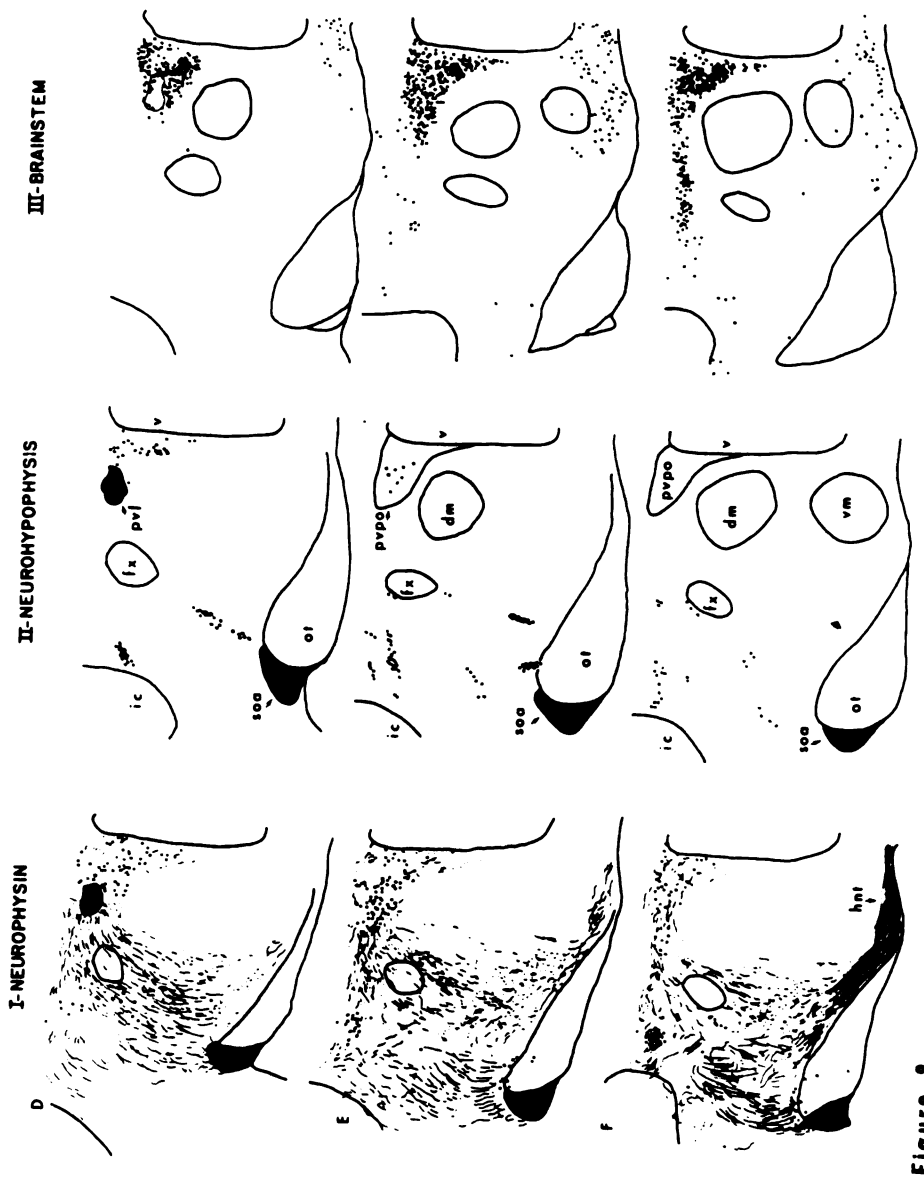
I-NEUROPHYSIN
II-NEUROHYPOPHYSIS
III-BRAINSTEM
D
E
F
ic
pvl
lx
v
soo
ol
pvpo
dm
vm
hnl

Figure 8

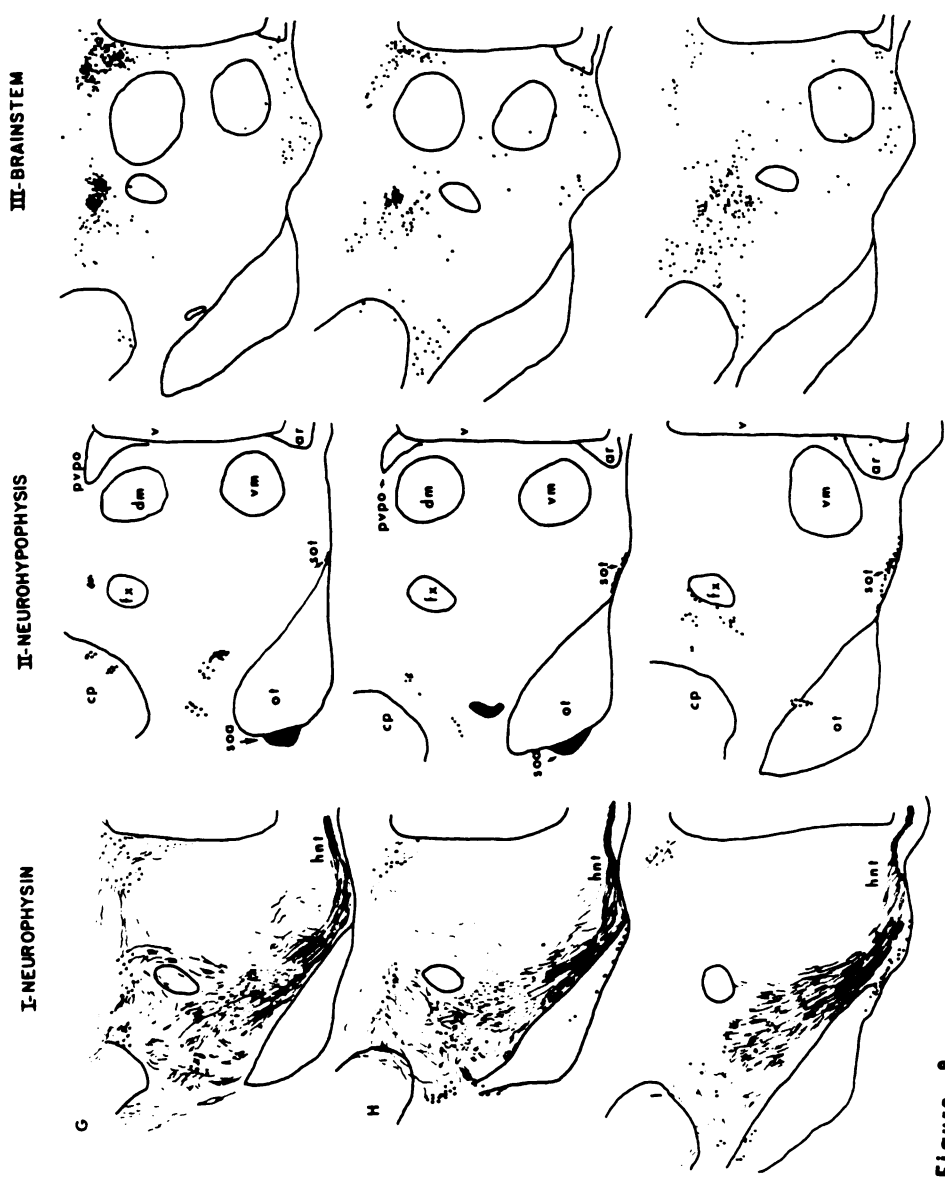
I-NEUROPHYSIN
II-NEUROHYPOPHYSIS
III-BRAINSTEM
G
H
I
cp
ix
dm
vm
pvpo
v
ar
sol
ol
soo
hnl

Figure 8

component of the neurohypophysial tract. In most animals the internal layer of the median eminence, which contains neurohypophysial-projecting axons, exhibited dust-like particles when BDHC or TMB was used as the chromogen.

In five rats it was determined that HRP had spread to the portal vasculature of the MEex since HRP was found in tanycytes and/or arcuate neurons. Furthermore, varying amounts of extracellular HRP were seen in the arcuate nucleus and laterally adjacent regions. Since the distribution of labelled pv cells in these rats was similar to that observed in animals receiving vascular injections, the results of these two groups are considered below under "Vascular injections."

For neurohypophysial injections the main effect of varying survival time and injection size was on the amount of reaction product evident in the labelled cells. For example, a rat receiving 1 µl of HRP and surviving 48 hr exhibited several solidly filled neurons (Keefer, 1978). In contrast, a much smaller injection (0.15 µl) followed by the same survival time resulted in a restriction of the reaction product to a small number of granules largely confined to somata. In some animals the adenohypophysis also contained HRP reaction product. In these rats the pattern of uptake seemingly differed from that following neurohypophysial injections only if accompanied by spread of the HRP to the arcuate-MEex region.

Brainstem/spinal cord afferents. Large (0.5 µl) single or multiple injections were placed in the lower medulla (Figure 9) or spinal cord in an attempt to label as many pv neurons as possible which might project to or through these regions. Since transected

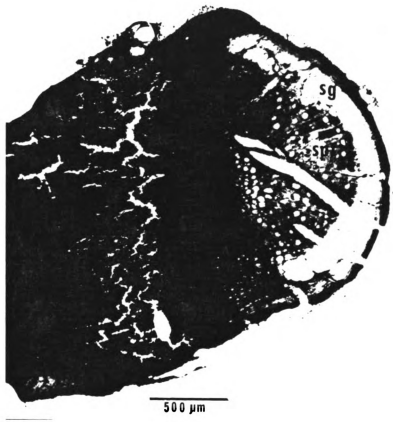

Figure 9. A low power photomicrograph of the lower medulla showing the dense distribution of reacted HRP (darkened area) 48 hr after a 0.5 µl injection into rat 34179. The distribution of labelled cells resulting from this injection is illustrated in Figures 4-7D and in Figure 8 III. The section was cut at 60 µm, reacted with H-Y and counterstained with thionine.

fibers are known to incorporate and transport HRP (e.g., Bunt, Hendrickson, Lund, Lund and Fuchs, 1975; Herkenham and Nauta, 1977; Halperin and Lavail, 1975), in one rat the cervical spinal cord was hemisected with fine tungsten wire at C1-C2 and two 0.5 µl injections, one medial and one lateral, were placed at the point of severance 1 mm lateral to the midline and about 1 mm below the cord surface. Another rat received identical treatment, except that the injections and hemisection were placed between T3 and T4. The pattern of uptake in rats receiving spinal cord or brainstem injections was nearly identical. In general, the intensity and number of labelled cells from brainstem injections were greater. The representative pattern of this labelling is illustrated in Figures 4-7D and 8 III, which depict the ipsilateral distribution of labelled hypothalamic neurons following a large (0.5 µl) injection into the caudal medulla (rat 34179, also see Figure 9). A lesser number of marked cells was present contralaterally as well, but spread of the HRP in most cases prevents one from determining whether a true contralateral projection is present.

Labelled neurons were found throughout the rostrocaudal limit of the pv, but only a few pvm or pvl cells were labelled. These latter cells were nearly always located at the edge of these subnuclei (Figures 5 and 6D). Rostrally, most labelled neurons were found on the dorsal edge of the pvm and in the dorsomedial parvocellular area (Figure 5D). Scattered marked cells were present lateral to the ac in the bed nucleus of the stria terminalis, dorsolateral preoptic area and along the medial edge of the caudate-putamen, but no labelled cells were found in the ac (Figure 4D). A few cells transporting HRP were located just rostral to the pvm in the anterior parvocellular

zone. Many of these are medium-large (16-18 μm) in size, with extensive processes projecting ventrally in most cases. A few very small cells (<10 μm) without visible processes were lightly labelled in this region as well. Near the pvl labelled neurons were clustered ventromedially and in the dorsomedial cap, with a few scattered HRP-positive cells lying immediately medial to this subnucleus (Figure 6D). The HRP-positive cells at this level are mostly of a medium size, with smaller labelled cells intermingled among these. A few marked cells border the medial, dorsal and ventromedial edges of the pvl.

Caudally, the pvpo has by far the greatest concentration of labelled neurons in the pv (Figures 7D; 8III E-I) regardless of the size or location of the injection within the brainstem/spinal cord. Several of the labelled pvpo cells are fusiform and large (between 20 and 25 μm), especially those in the dorsal and lateral aspects of this subnucleus. Medially and ventromedially in the pvpo the labelle cells appeared noticeably smaller. Medium sized neurons appeared to make up most of the labelled population. As can be seen in Figure 7D, the pvpo is virtually filled with HRP-positive cells following a large injection into the lower brainstem. Only on the medial aspects were labelled elements sparse. The apex of the pvpo triangle constitutes a band of horizontally oriented, labelled neurons which stretches laterally over the fornix to the medial edge of the cerebral peduncle, where a second accumulation of HRP-positive cells resides (Figure 8III F, G). Caudally this cluster of labelled cells expands into much of the dorsolateral hypothalamus, with several marked cells seen lying around the fornix (Figure 8III I). Although not nearly so large in number, perifornical cells were also labelled after neurohypophysial injections and are presumably a component of the paraventricular

accessory nucleus (Bandaranayake, 1971; also called the posterior fornical nucleus by Peterson, 1966). Labelled pvpo cells decrease in number at these levels as they assume a position more dorsal to the 3 V (Figure 8III G, H and I). Other hypothalamic cells labelled by brainstem and spinal cord injections resided in the lateral hypothalamus or were scattered in a ventral band which extends from beneath the 3 V to a lateral position beneath the ventromedial hypothalamic nucleus.

Smaller, multiple injections (0.1-0.2 µl) in three other rats were made in the region of vago-solitary complex with spread of the HRP to immediately adjacent areas. These injections resulted in a pattern of labelling similar to that described for larger injections, except fewer cells were labelled. In addition, very few cells were found in the rostral portions of the pv in these animals. Relatively fewer cells were found contralateral to the injection site in contrast to larger injections. While the injection sites appeared not to have extended bilaterally in these animals, the long (48 hr) survival times could have allowed for removal of the lower concentrations of HRP that may have been present earlier on the side opposite the injection. Smaller injections were made with micropipettes and therefore may have damaged fewer fibers in passage than those made with a 31 ga needle. The rat receiving a CSF control injection exhibited no labelling following a 48 hr survival time.

Many labelled pvpo neurons possess processes which emerge from each end of their elongated somata. Some cells are obviously multipolar with branching dendrites. Such profiles were rarely observed in filled pvl or pvm neurons. It is difficult to determine from this material if this represents a real cytoarchitectural difference,

since the packing density is great in the pvm and pvl compared to the pvpo.

Summary of brainstem/spinal cord and neurohypophysial injections. In general, the pv neurons projecting to the neurohypophysis or brainstem/spinal cord are relatively segregated from one another into cytoarchitecturally distinct subnuclei, although zones of overlap were noted. These results are summarized in Figure 10. Neurohypophysial afferents arise primarily from the pvl and pvm, with scattered dorsomedial cells also contributing to this projection; cells projecting to the brainstem/spinal cord are located ventromedially and dorsomedially to the pvl, dorsally and rostrally from the pvm and most densely in the pvpo. The dorsomedial contingent of labelled cells resulting from brainstem/spinal cord injections is concentrated in the dorsomedial cap.

Rostrally the dorsomedial zone, largely *excluding* the dorsomedial cap, appears as a zone of overlap, with cells in this area projecting to both the neurohypophysis and brainstem/spinal cord. LIkewise, the zone ventromedial to the pvl appears to contain both (or a single) type(s) of neuron(s). Further studies will be needed to determine if these zones of overlap include cells with collateral axons. Also, the identical distribution of cells projecting to the brainstem and spinal cord suggests that collateral innervation of these areas is likely.

The ac apparently connects with the neurohypophysis but no uptake was present in this nucleus after brainstem/spinal cord HRP injections. Whereas ac and pv neurons labelled subsequent to neurohypophysial injections were mostly magnocellular, pv cells of all sizes were commonly found to project to the brainstem/spinal cord.

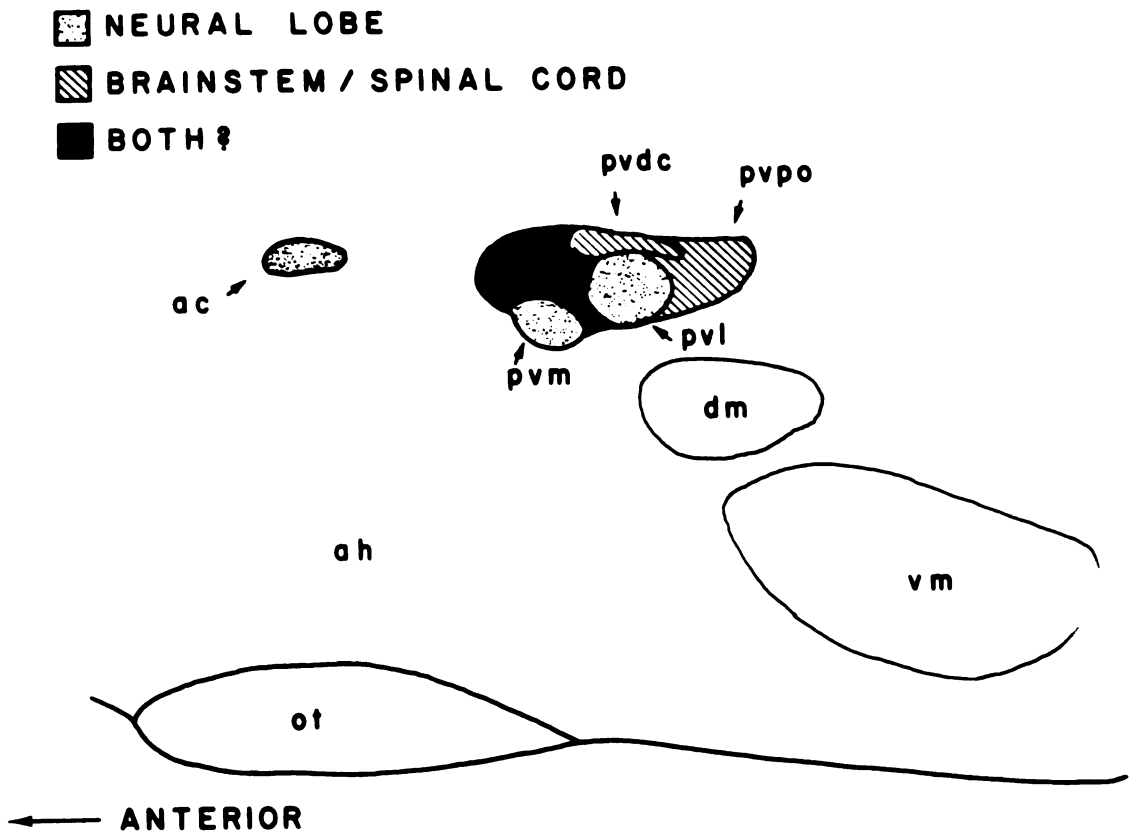

Figure 10. Schematic representation of the ac and pv in sagittal section depicting the relationship of these nuclei with the neurohypophysis and brainstem/spinal cord. The nuclei have been divided on the basis of the efferent projections to these areas. "Both?" indicates that these areas contain cells which project to both places, but whether individual cells are responsible for this dual innervation is unknown.

Vascular injections. Retrograde labelling in the pv resulting from intrajugular HRP injections was most significant, in terms of intensity and number of labelled cells, after 12 and 24 hr survival times. Light labelling was clear at 6 but not at 1/2 hr post-injection, and was still evident at 48 hr survival.

As mentioned previously, the pattern of pv labelling after blood injections was similar to that observed following neurohypophysial injections from which HRP had spread to the arcuate-MEex region. Following both types of injection a diffuse, granular reaction product can be seen covering the basal region of the arcuate nucleus and extending laterally (Figure 11). From both types of injection labelled magnocellular neurons with a distribution similar to that observed after precise neurohypophysial injections were evident in the pv. In addition, a considerable number of parvocellular neurons had also transported the enzyme. Figures 12 through 14, which illustrate the distribution and character of these small cells from a rat receiving a neurohypophysial injection with spread to the arcuate-MEex region, are relevant to the results of vascular injections as well. The labelled parvocellular neurons were found largely in the medial portions of the pv. These small cells may provide a pv connection with the MEex, but it cannot be ruled out that uptake was due to the involvement of the arcuate region. In rat 051078, which exhibited the largest number of labelled parvocellular neurons, cell counts in alternate sections through the pv revealed that parvocellular neurons accounted for approximately 20% of the labelled cell population (Figure 13). In contrast, small cells were rarely labelled after precise neurohypophysial injections.

Figure 11. Illustrations and photomicrographs of coronal sections showing the presence of HRP in the arcuate-MEex region following vascular (A and B) or neurohypophysial injections (C and D) which involved spread of the enzyme. In A and C, the approximate areas photographed in B and D, respectively, are enclosed by rectangles. In A and C, the arrow points to the median eminence, which has been added to the drawing in C due to its loss in tissue processing. In B and D, lateral arrowheads point to the arcuate region. In B the middle arrowhead points to the MEex. Note in the darkfield photomicrographs in B and D the refractivity of the diffusely distributed TMB reaction product in the arcuate region. The distribution of labelled cells resulting from the injection shown in D is illustrated in Figures 12-14, taken from rat 051078. Bar = 500 µm.

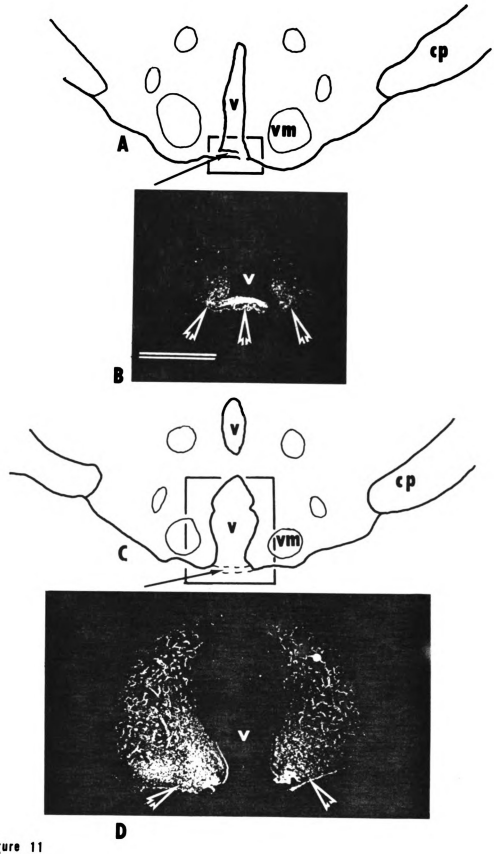

Figure 11

Figure 12. Diagram from tracings of coronal sections showing the distribution of small (≤14 μm, long diameter) and larger (>14 μm) cells following a neurohypophysial HRP injection with spread of the enzyme to the arcuate-MEex region. Sections through the pvm (A), pvl-pvdc (B) and pvpo (C) are represented and were taken from rat 051078. Note the primarily medial distribution of small cells and the lateral distribution of larger cells. The arcuate-MEex region of the rat represented is shown in Figure 11C. The numerical distribution of the labelled cells represented can be found in Figure 13. Filled circle = large cell; x = small. Blackened areas in A and B represent the dense concentration of predominantly large HRP-labelled neurons in the pvm and pvl, respectively. In B, the area approximately enclosed by the rectangle is shown in the photomicrograph of Figure 14.

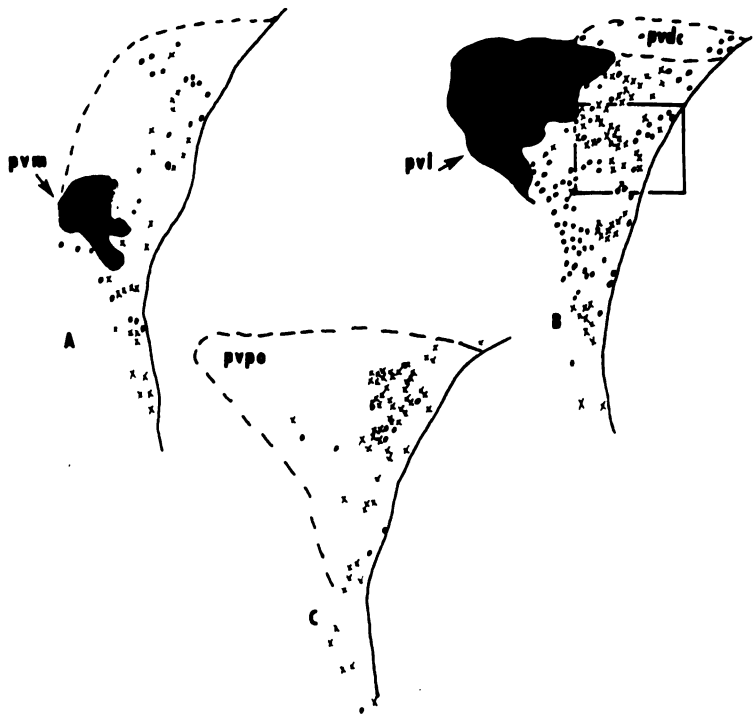

Figure 12

Figure 13. The numerical distribution of large and small HRP-positive pv cells resulting from a neurohypophysial injection with spread of the enzyme to the arcuate-MEex region. Counts were made in alternate, 60 µm sections reacted with TMB and counterstained with neutral red. On the horizontal axis, each successive number represents a section 120 µm caudal to the previous section beginning with 1, which is the most rostral section through the pvm. Beneath each section number the constituent subnuclei in that section are given. The medial parvocellular zone is found in all sections (see Figure 12). Note the large number of cells with a long diameter greater than 14 µm and the substantial contingent of smaller cells. The distribution of labelled cells from the same rat (051078) is illustrated in Figure 15. The arcuate-MEex region of this rat is shown in Figure 11C.

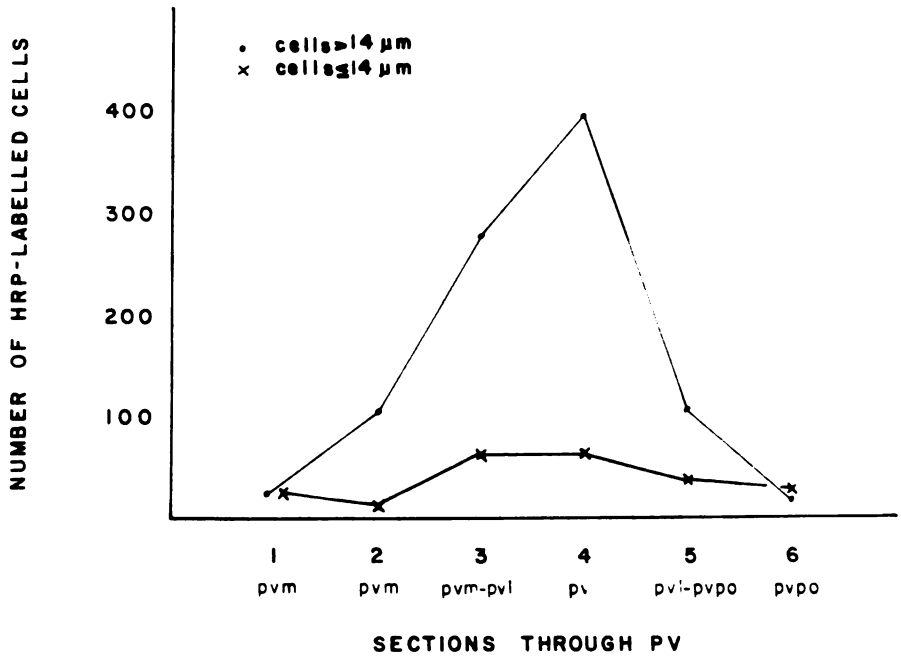
• cells>14 µm
× cells≤14 µm
NUMBER OF HRP-LABELLED CELLS
400
300
200
100
1
pvm
2
pvm
3
pvm-pvl
4
pv
5
pvl-pvpo
6
pvpo
SECTIONS THROUGH PV

Figure 13

Figure 14. A high power photomicrograph taken from approximately the same area of the pv enclosed by the rectangle in Figure 12B. Parvocellular neurons (arrowheads) are seen labelled in addition to magnocellular neurons (arrows). Note that reactive processes are not prevalent extending from small labelled cells. Taken from rat 051078, which received a neurohypophysial injection with spread of the enzyme to the arcuate-MEex region (see Figures 11-13). Taken from a 60 µm section reacted with TMB and counterstained with neutral red.

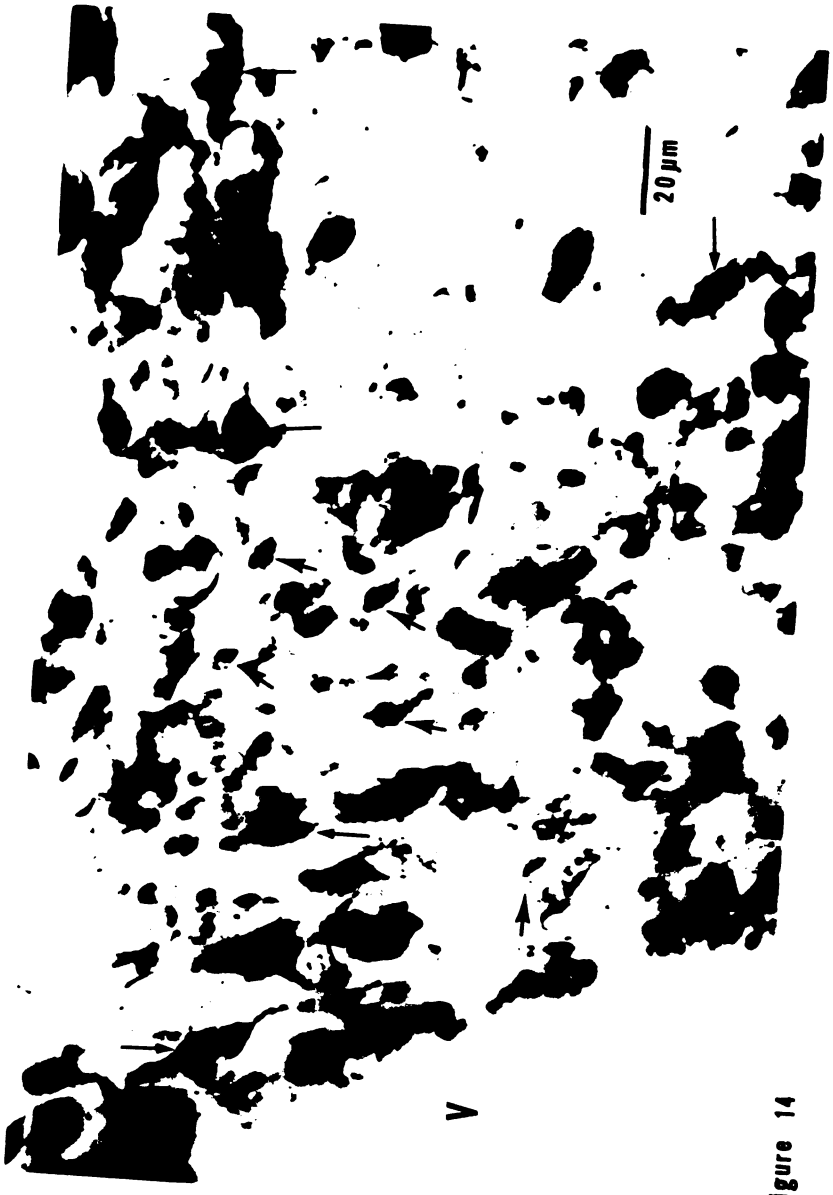

Figure 14

Labelled parvocellular elements rarely displayed reactive processes (Figure 14). Few of these cells appeared densely filled; most often granules were observed scattered in the scant cytoplasm. The labelled parvocellular neurons are most often situated vertically, and they appear to be morphologically similar to more ventrally located labelled periventricular cells which also can be seen after these types of injections.

Vascular injections also resulted in the labelling of cell populations not observed after either type of neurohypophysial injection (i.e., those with or without spread to the arcuate-MEex region). For example, the labelling of brainstem cranial nuclei indicates that the results of neurohypophysial injections were not due to a general spread of HRP throughout the vascular system. Interestingly, a few labelled cells were observed in nucleus triangularis of the septum, where NP-positive cells reportedly have been seen (Sofroniew and Weindl, 1978). The pattern of cell labelling in the ac and adjacent periventricular magnocellular nuclei was similar to that observed in rats receiving precise neurohypophysial injections.

Amygdalar afferents. In contrast to the large number of cells in the pv found to project to the neurohypophysis and brainstem/spinal cord, few HRP-positive cells were located in the pv following even the largest of injections into the amygdala. Axoplasmic transport was not generally impaired in these rats since large numbers of labelled cells were present in other forebrain structures.

Despite extensive spread of the HRP in all twelve animals, labelled pv neurons were found in only four rats. The range of marked cells across animals was from three in a rat receiving a 0.1 µl

injection with the needle tip placed at the junction of basolateral and basomedial nuclei, to 65 labelled cells in rat 49579. The latter rat received a total of 1.55 µl of HRP utilizing five penetrations and eight delivery sites. The entire temporal lobe and much of the dorsally adjacent neocortex, lateral hypothalamus and supraoptic nucleus contained reaction product. A few cells were labelled in two other rats with single placements centered in the lateral (0.2 µl) or cortical (0.15 µl) nucleus. An example of an injection confined to the amygdala is shown in Figures 15 and 16A.

As can be seen in Figure 17, the labelled pv cells following amygdalar injections were distributed mainly, though not exclusively, in the anteromedial parvocellular zone. These cells are typically small-medium in size and vertically oriented, appearing aligned with the periventricular stratum (Figure 18). An occasional large cell was seen in the pvl and pvm (Figure 17B and C). The most convincing example of a labelled magnocellular neuron is shown in Figure 19A, taken from rat 43479, which received an injection centered in the endopiriform nucleus but which spread to the adjacent lateral and basolateral nuclei and piriform cortex (Figures 15 and 16A). This neuron was actually outside of the densely packed pvm and pvl, being medial to the latter (Figure 19B). Another magnocellular cell which had transported HRP was present in this animal in the medial pvpo.

The most dorsomedial contingent of labelled cells shown in Figure 17 appeared to be a lateral extension of the medianus preoptic nucleus and adjacent thalamus. The latter cells lie near the dorsal apex of the third ventricle and caudally were more intensely reacted than many adjacent dorsal and dorsolateral neurons of the nucleus reuniuns. Of further interest were the few marked cells lying between

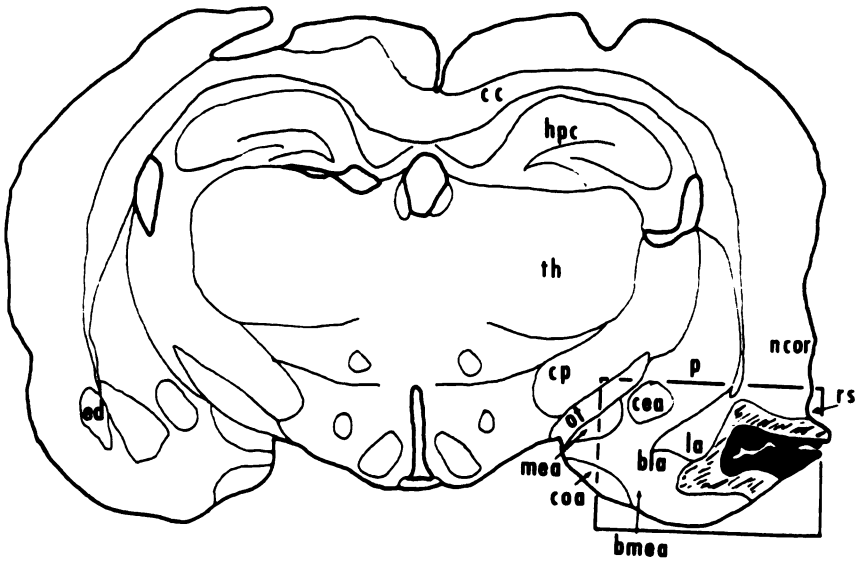

A

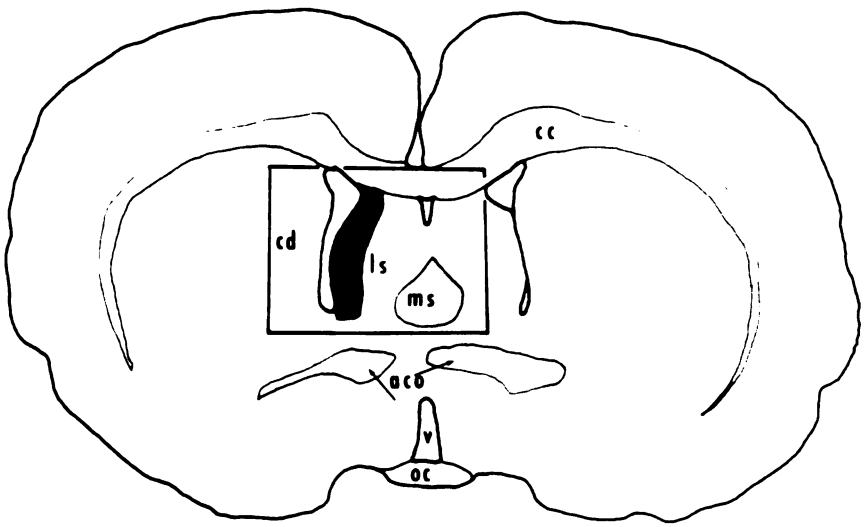

B

Figure 15. Diagrams of tracings from coronal sections illustrating the central location of HRP injection sites in the amygdala (A; rat 43479) and septum (B; rat 54679). The areas approximately enclosed by the rectangles are shown in the photomicrographs of Figure 16A and B, respectively. From 60 µm sections reacted with H-Y and counterstained with thionine. See Figure 16 for further details.

Figure 16. Photomicrographs of HRP injection sites (darkened areas) in the amygdala (A) and septum (B) which were illustrated in Figure 15. The labelled magnocellular neuron exhibited in Figure 19 resulted from the 0.2 µl injection shown in A, which was centered in the endopiriform nucleus. Spread is evident into the adjacent basolateral and lateral nuclei, and in the piriform cortex. The rat represented (43479) survived 44 hr post-injection. In the photomicrograph of the septum in B, the core of a 0.2 µl injection into the lateral septal nucleus is shown. This rat survived 36 hr post-injection and the hypothalamic distribution of labelled cells resulting from this injection is shown in Figure 20 (rat 54679). Taken from 60 µm sections reacted with H-Y and counterstained with thionine.

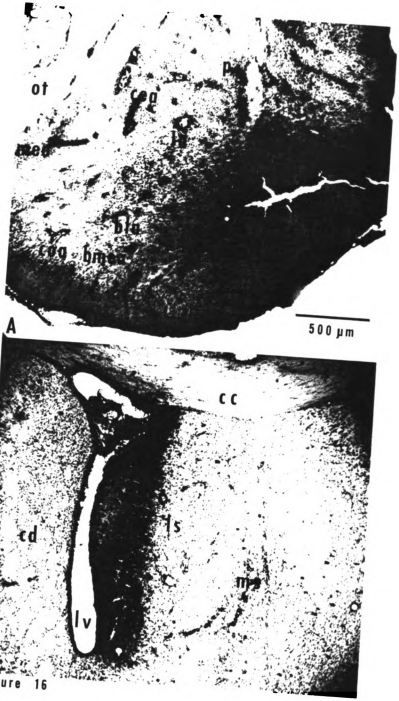

Figure 16

Figure 17. Diagram from tracings of coronal sections showing the ipsilateral distribution of HRP-labelled cells in the major pv subdivisions subsequent to multiple injections into the amygdala totalling 1.55 µl (rat 49579). These injections covered all of the nuclei of the amygdala and several adjacent structures. Note the relatively large number of labelled cells in the anterior parvocellular zone (within dashed lines in A) and dorsomedial proximity of these cells to neurons outside, but adjacent to, the pv. Many of these latter cells appear to be an extension of the medianus preoptic nucleus and adjacent thalamus. Note also the scattered, labelled cells in pvm (B), pvl (C) and pvpo (D). This rat survived 36 hr post-injection. The area enclosed in the rectangle in A approximates the area shown in the photomicrograph of Figure 18.

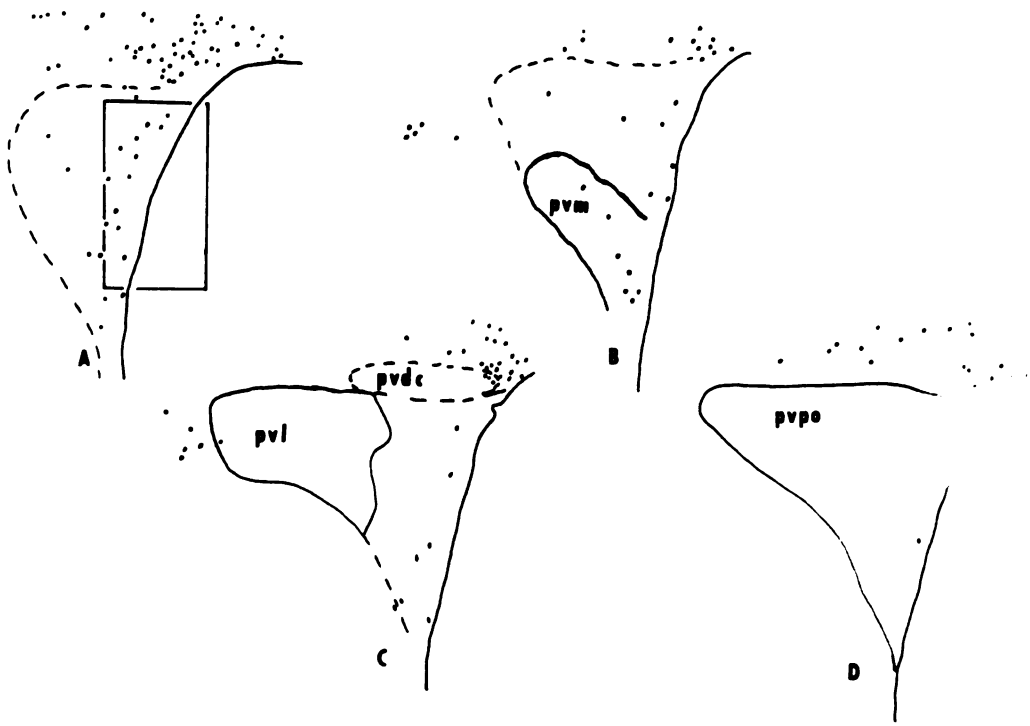

Figure 17

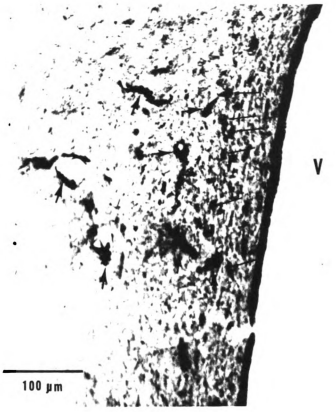

Figure 18. Photomicrograph of the area approximately enclosed by the rectangle in Figure 17A. Shown are medial HRP-labelled cells (small arrows) in the anterior parvocellular zone of the pv following injections into the amygdala. In all cases the labelling in this area is relatively light and difficult to see against the background of anterogradely transported HRP. Large arrowheads point to the artifactual deposits of TMB reaction product, most often associated with blood vessels. Note the vertical alignment of the labelled cells with the periventricular stratum. From a 60 µm section reacted with TMB and counterstained with Safranin-O. Represented is rat 49579, which survived 36 hr following multiple injections into the amygdala totalling 1.55 µl.

Figure 19. A high power photomicrograph of an HRP-labelled magnocellular neuron (large arrowhead) and its location in the pv (B) are shown. The cell's long diameter exceeds 20 µm. Note the cell's location just medial to the pvl (B). In A, small arrows point to artifactual deposits of TMB reaction product. In B, small arrows point to the "tear" seen in A. These illustrations were taken from a 60 µm coronal section reacted with TMB and counter-stained with Safranin-O. Represented is rat 43479, which received a 0.2 µl injection (see Figures 15 and 16A) and survived 44 hr post-injection.

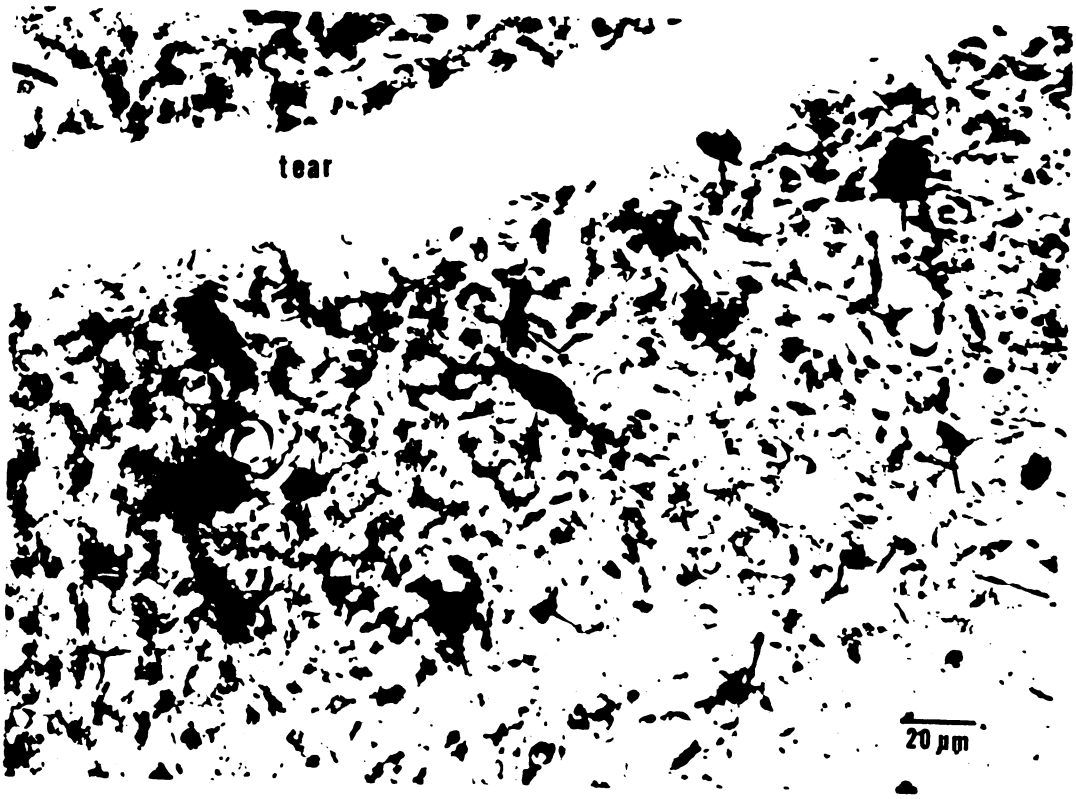

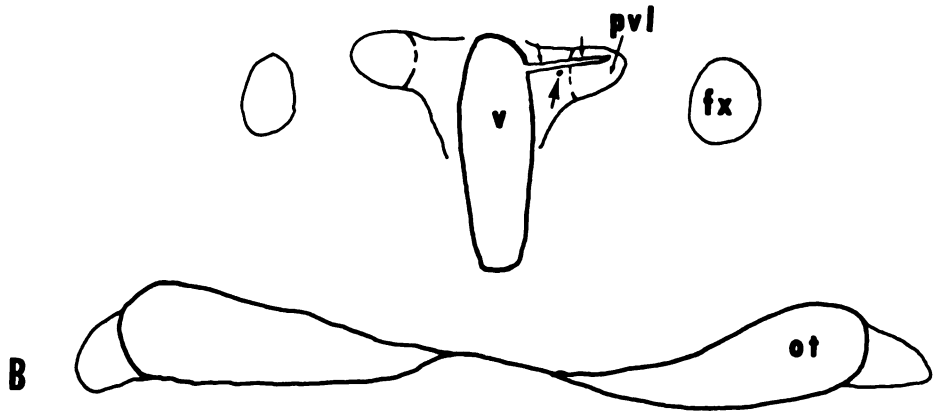

Figure 19

the pvl and the fornix (Figure 17C). A similar group of neurons, though larger in number, was more heavily labelled following septal injections (see below).

It might be argued that spread of the HRP outside the amygdala in rat 49579 accounts for the relatively large amount of pv labelling (Figure 17). However, all of the adjacent structures were involved in varying degrees in many other animals wherein no labelled pv cells were seen. Since the labelled elements were uniformly ipsilateral to the injection site, ventricular spread apparently cannot account for this result.

In several animals neurons of the supraoptic nucleus appeared to be lightly labelled on the side ipsilateral to the injection. In some rats this result may be due to the spread of HRP to this nucleus; in other rats the injection boundaries are less clear. At this ti the most parsimonious conclusion would be that supraoptic neurons may have taken up the HRP at somal or dendritic membrane sites.

In conclusion, amygdalar afferents from the pv may arise from all of the major pv divisions, but most cells were found in the medial aspect of the nucleus. Cells of all sizes may participate in this connection, but the number of cells is small relative to that involved in neurohypophysial and brainstem/spinal cord pathways.

Septal afferents. Although significantly more hypothalamic neurons were labelled by septal compared to amygdalar HRP injections, the contribution of the pv was still relatively small. A substantial number of labelled neurons were found in areas immediately adjacent to the pv, and in five rats scattered, labelled cells were evident in many of the pv subdivisions. Injections into the lateral septal

nucleus resulted in the labelling of the most hypothalamic cells in general, including the pv. The lateral septal nucleus was injected in three animals. Medial septal injections also resulted in pv labelling. These injections, made in three rats also, involved the fimbrialis and triangularis nuclei as well. In two rats the septum was missed and the injections were placed into either the rostral hippocampus or fimbria. No pv labelling resulted from these injections.

An example of a 0.2 µl HRP injection into the lateral septal nucleus is shown in Figures 15 and 16B. The distribution of cells retrogradely labelled 36 hr after this injection is shown in Figure 20. The largest number of reactive cells was located in the anterior parvocellular zone, adjacent to labelled cells in the area wedged between the pv and anterior portion of the thalamic paraventricular nucleus and the parataenial nucleus (Figure 20B). Cells of these latter nuclei were also labelled. Labelled pv cells at this level range from small (the majority) to large (a few). More caudally, scattered cells were seen dorsal and medial to the pvm. A few cells lie within the boundaries of this subnucleus (Figure 20D). Near the pvl several marked cells were evident at the dorsal, ventral and lateral borders of this subnucleus. A few labelled neurons were found within the pvl (Figure 20E). Likewise, a few large labelled neurons border the lateral and ventral aspects of the pvpo and occasionally can be found in this subnucleus (Figures 20G, 21H). All observed pv labelling was ipsilateral to the injection site.

Particularly conspicuous following lateral septal injections were the labelled cells between either the pvl or pvpo and the fornix (Figure 21). Caudally this cluster of cells was seen near a large

Figure 20. A diagram constructed from tracings of coronal sections illustrating the ipsilateral distribution of HRP-labelled, hypothalamic cells following a 0.2 µl injection into the lateral septal nucleus (see Figures 15 and 16B). Note the dense labelling in the anterior parvocellular zone (B-D). A few labelled cells are located in the pvm (D), pvl (E) and pvpo (G-I). Note also the close proximity of labelled cells outside the pv, particularly the group lateral to the pvl-pvpo (F-I). The area enclosed by the rectangle in G approximates the location shown in the photomicrograph in Figure 21. From rat 54679, which survived 36 hr post-injection.

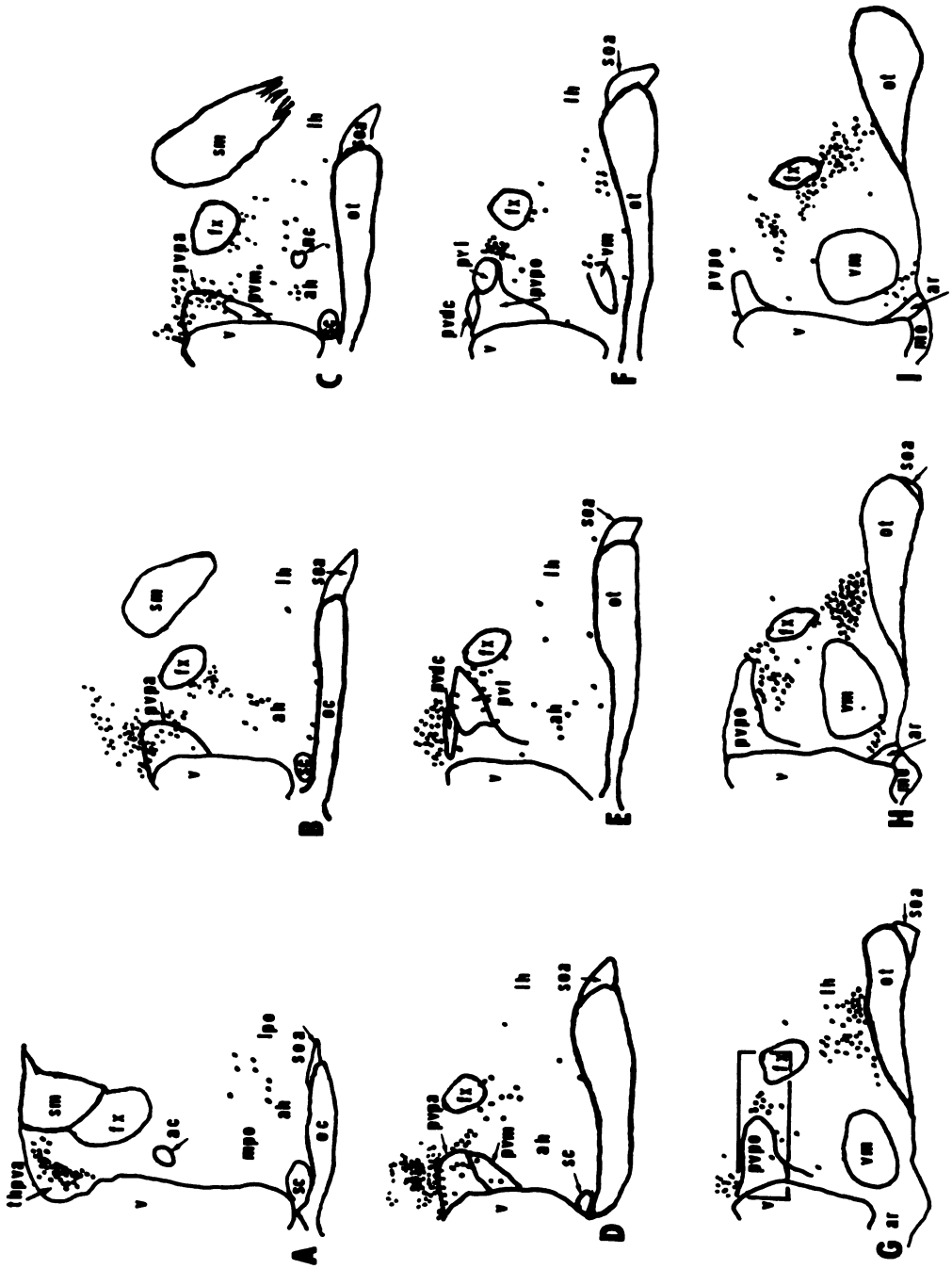
A
B
C
D
E
F
G
H
I
sm
lx
Qac
mpo
lpo
soa
oc
sc
ah
lh
ol
pvpa
pvm
pvi
pvdc
pvpo
vm
ar

Figure 20

Figure 21. A photomontage illustrating HRP-labelled cells in the pvpo (small arrows) and the laterally adjacent area (large arrowhead) after a 0.2 µl injection into the lateral septal nucleus (see Figures 15 and 16B). The photomicrographs were taken approximately from the area enclosed by the rectangle in Figure 20G. Note also the dense band of anterogradely-transported HRP along the periventricular stratum, surrounding the fornix and ventrolateral to the pvpo. Other dark profiles in the pvpo are not labelled cells, but rather artifactually deposited TMB reaction product. Taken from a 60 µm section reacted with TMB and counterstained with Safranin-O. Represented is rat 54679, which survived 36 hr post-injection.

Figure 21

group of labelled neurons in the lateral hypothalamus (Figure 20I) and in one rat the two cell groups appeared to be continuous at this level.

The distribution of labelled pv cells resulting from medial septal injections was generally similar to that described for lateral injections. However, fewer labelled cells were found and uptake was observed bilaterally in two of these rats. Not nearly as many hypothalamic neurons were labelled from medial compared to lateral injections. Again, the cell size of reactive neurons ranged from small to large after medial injections.

Ventricular spread was evident in four animals. Two of these received medial, two lateral injections. In these rats the ependymal cells along the dorsal two-thirds of the 3 V had accumulated the HRP. However, in three of these rats the labelling in the pv occurred ipsilateral to the injection site. This result includes one rat with an injection into the medial septal nucleus which was centered off the midline. In the fourth rat with apparently the largest degree of ventricular spread, magnocellular neurons of the pvm, pvl and the supraoptic nucleus were lightly labelled, bilaterally. This labelling was likely due to ventricular spread of the HRP. This rat received a 0.2 µl injection into the medial septal nucleus.

In conclusion, those neurons observed to project to the septum appeared to reside primarily in the anterior parvocellular zone, but a few cells were definitely located in the pvm, pvl and pvpo. It may be significant that the cells seen in these latter divisions were most often located just within their borders, indicating that the overlap of these neurons with those projecting to the neurohypophysis may not be substantial.

Summary of vascular, amygdalar and septal injections. The labelling observed following vascular injections and neurohypophysial injections with spread of the HRP to the arcuate-MEex region indicates that medial parvocellular pv neurons may project to either or both of these areas. It is of course possible that magnocellular neurons projecting to the neurohypophysis project to these regions also. Experiments attempting to more conclusively answer this question were attempted by approaching the pituitary ventrally and either removing it or ligating the stalk (which contains neurohypophysial fibers) before administering the HRP. A consistent disruption of the blood supply during surgery prevented adequate fixation in these rats and no reaction product was observed in any of the animals.

In contrast to that seen following brainstem/spinal cord and neurohypophysial injections, little clustering of pv neurons projecting to the amygdala and septal area was observed. Most cells projecting to these areas were located in the anterior parvocellular zone, dorsomedial to the pvm. Importantly, however, some unequivocal cases of large cell labelling were observed in the pvm, pvl and pvpo. In all instances the cells in these areas were few and distributed among many unlabelled neurons.

Distribution of neurophysin (NP)

The distributions of NP-containing cells and fibers were mapped in order to determine their relationship with the various pv subnuclei. The antisera used in this study have been shown to cross-react with both OX- and VP-neurophysins in the rat (Seif et al., 1971; Robinson et al., 1971) and thus provide a general picture of the distribution of the primary pv neurohypophysial hormones (OX, VP and their

neurophysins). It is important to emphasize that lack of a positive reaction cannot be taken as evidence of a lack of hormone within any one cell. Nevertheless, regional variations within animals may provide further insight into the differences or similarities among the subnuclei studied. For comparison, selected coronal sections of NP material (from rat NP-1, in which the rat NP was utilized to generate the antiserum) and HRP-injected brains (from brainstem and neurohypophysial injections) were traced and shown together in Figure 8. In general, there was good agreement between the bovine and rat NP-generated antisera employed regarding the location of reactive cell bodies. However, the antisera generated against the rat NP resulted in a finer distribution of fibers and a greater staining intensity. No staining in control sections was observed, where phosphate-buffered saline was substituted for the primary antisera.

Anterior commissural nucleus (ac). The ac contains a considerable number of darkly staining, NP-positive perikarya throughout its extent (Figures 4B, 8I A). Axon trajectories from this nucleus (in the form of thin, beaded fibers) were much less distinct than those from the pv or supraoptic nuclei; no clear fascicle was seen emerging from the nucleus. Laterally extending beaded fibers were observed in scattered batches coursing under the fornix, whereas others were seen turning dorsally. None of these could be followed continuously for a great distance. A few NP-positive cells at this level were seen sandwiched between the stria meduallaris and fornix, while others lay among a group of NP-positive fibers within the stria terminalis (Figure 8I A).

Thick processes (putative dendrites) could be seen extending medially, but few processes were seen emerging directly dorsal or ventral from the ac. In counterstained sections, several small and few larger cells were nonreactive. Of the NP-positive cells that were clearly sectioned through the nucleus (i.e., exhibiting a nucleolus), few measured less than 15 µm; most measured 17-20 µm along the long diameter.

Large, darkly stained, NP-positive neurons were also seen lying adjacent to the 3 V wall just medial to the ac (Figures 4B, 8I A). These periventricular cells can be found scattered along the rostrocaudal extent of the 3 V, but the conglomeration medial to the ac is the most conspicuous group. The cells of this conglomeration decreased in number caudally, so that only a few remained at the level of the pvm. This group is not considered as part of the ac since the cells appeared to be part of an extensive periventricular NP-containing system and were separated from the ac by a cell sparse zone.

Medial magnocellular paraventricular nucleus (pvm). The pvm also contains many NP-positive perikarya (Figures 5B, 8I B). In counterstained material, however, a few unreactive magnocellular neurons were apparent scattered throughout this subnucleus. A few labelled cells, including some in the dorsomedial cap, were found dispersed dorsomedial to the pvm. The long axis of most NP-positive pvm cells exceeds 20 µm. The dorsomedial elements are of a similar size. Rarely, a parvocellular neuron appeared to contain reaction product. The distribution of NP-positive pvm cells correlates well with that of cells afferent to the neurohypophysis. Also, HRP-labelled cells

from all injections coexist with NP-containing cells in the area dorsomedial to the pvm.

Most NP-positive beaded axons from the pvm were seen to course ventrolaterally beneath the fornix in a wide sheet (Figure 8I B). A few fibers at this level were noticeable atop the fornix, but their origin was not obvious. Thick, medial processes were seen emanating from the clustered pvm cells as was evident in the ac, but such processes were not nearly as prevalent as in the latter nucleus. Neither beaded axons nor thick processes were commonly observed emerging directly ventral or dorsal to the pvm.

Lateral magnocellular paraventricular nucleus (pvl) and dorsomedial cap. Many cells occupying the transition zone between the pvm and pvl were reactive. Referring again to Figure 6C and D, one can see that this zone also contains cells which project to the neurohypophysis and/or to the brainstem/spinal cord. Caudally through the main body of the pvl (Figure 6B), which was concentrated with large NP-positive cells, the density of reactive cells in the ventromedial zone declined significantly. The majority of the ventromedially located, NP-negative neurons are small-medium in size. On its medial aspect the pvl is bordered by a population of non-reactive cells which again are mostly small, yet a few unstained magnocellular neurons were observed. Adjacent to the pvl, dorsomedial cap cells were largely non-reactive, but a few medium sized NP-positive cells were seen here as well (Figure 6B). A loose organization of magnocellular NP-positive neurons and rarely reactive parvocellular neurons were located throughout the zone medial to the pvl. The great majority of reactive pvl neurons range in size from 18-25 μm.

Axons arising from the pvl were topographically distributed, with dorsal cells giving rise to beaded fibers which coursed over the fornix to turn ventrally or, in some cases, project toward the cerebral peduncle (Figure 8I C and D). Ventrally located somata have fibers projecting ventrolaterally beneath the fornix to join the mass of fibers of the neurohypophysial tract over the optic tract. Thick processes extended a short distance medially or followed the ventromedial contour of the pv. A few thick processes were observed extending dorsally or ventrally from the pvl.

Posterior paraventricular nucleus (pvpo). Caudally the density of NP-positive cells diminished in concert with overall cell numbers in the pv. However, many reactive neurons were seen in the pvpo (Figure 7B). These cells were oriented mediolaterally, and their long axes frequently measured greater than 22 μm, but less than 25 μm. The number of pvpo cells which are NP-positive is far greater than the few pvpo neurohypophysial-projecting cells but is less than the number of brainstem/spinal cord projecting cells. Nevertheless, the triangular outline of the pvpo and its rostrocaudal extent as revealed in Nissl-stained material and in brainstem/spinal cord HRP-injected brains was matched by the distribution of NP-positive elements. This correspondence includes the group of accessory cells referred to earlier which lies dorsal and dorsolateral to the fornix and which appears to be a lateral extension of the pvpo (Figures 2, 8I G and H). Beaded fibers from the pvpo followed the same initial course as those from the caudal pvl, with trajectories over and under the fornix. At more caudal levels the majority of these fibers appeared to pass over the fornix. Ventral and lateral to the fornix a meshwork of NP-positive

fibers was visible. Some of these fibers appeared to turn dorsally along the dorsomedial edge of the cerebral peduncle, while most axons appeared to turn ventrally. This seemingly random tangle of fibers appeared to consist of dorsomedially extending supraoptic axons, pvl fibers and pvpo fibers, the last of which are most likely turning caudally.

Thick medial and sometimes lateral processes of pvpo cells were prominent (Figure 7B). Most of these were oriented in parallel with the long axes of most pvpo cells, but an occasional thick process was seen to extend dorsally.

Summary of neurophysin (NP) results. Cells immunoreactive for either NP antiserum employed in this study are distributed in regions in the pv which largely correspond with the distribution of projection neurons. Thus, most neurohypophysial-projecting and many brainstem/spinal cord-projecting cells in particular probably contain NP. However, a considerable number of medium sized and small neurons project caudally, and to the septum and amygdala. Most cells of this size having a distribution similar to the small-medium projection neurons are not NP-positive. Thus, it seems likely that some pv neurons which project to the MEex and extrahypothalamically are not neurophysinergic. A procedure allowing the double-labelling of NP and retrogradely transported HRP could more definitively answer this question.

The most important result is that the pvpo and dorsomedial cap were found to contain NP-positive and extrahypothalamically-projecting cells, yet contain a paucity of cells projecting to the neurohypophysis. On the other hand, all of the areas observed to

contain cells which project to the neurohypophysis also have a considerable number of NP-positive perikarya. This would indicate a separation of neurohypophysial and brainstem/spinal cord neurophysinergic systems. The innervation of the septum and amygdala by NP-containing fibers could derive from the few magnocellular neurons seen to project to these areas. The large cells of this type located in the pvm and pvl might be expected to project to the neurohypophysis as well, due to the great concentration of HRP-labelled perikarya in these subnuclei after neurohypophysial injections.

Although NP-containing fiber trajectories differ along a rostrocaudal gradient, distinct bundles which might account for the differential innervation of the various structures studied could not be easily identified near the pv. Beaded fibers (putative axons) are distributed laterally in all the areas studied and thick processes (putative dendrites) are largely, although not exclusively, oriented medially.

General conclusions

It is suggested that the pv may be divided into at least five cytoarchitecturally distinct areas (subnuclei) which are related to the distribution of projection neurons and cells synthesizing NP (and thus OX or VP). Beginning rostrally, the dorsomedial portion of the 1) *medial parvocellular zone* contains mostly small cells, some of which project extrahypothalamically. The few large cells in this area probably contain NP and project to the neurohypophysis and/or the brainstem/spinal cord. The 2) *pvm* contains large cells, the great majority of which project to the neurohypophysis and contain NP.

A few *pvm* cells may project to the septum and amygdala. The continuing *medial parvocellular zone* at the level of the *pvm* contains small cells which may project extrahypothalamically and to the arcuate-MEex region; scattered large cells in this region contain NP and probably project to the neurohypophysis. The 3) *dorsomedial cap* contains a few NP-containing medium sized neurons and is filled with cells of the small-medium variety which project to the brainstem/spinal cord. A few cells of this area may project to the septum or amygdala. The 4) *pvl* is made up of large, NP-producing cells which project most discernibly to the neurohypophysis. A few *pvl* cells may project to the septum and amygdala. The continuing *medial parvocellular zone* at the level of the *pvl* contains small cells projecting to the arcuate-MEex region and outside the hypothalamus, most of which do not appear to contain NP. A few large, NP-producing cells in this area probably project to the neurohypophysis. The 5) *pvpo* contains cells of all sizes, most of which project to the brainstem/spinal cord. Medially within the *pvpo*, small cells may project to the arcuate-MEex region and extrahypothalamically, but do not contain NP. Large cells of the *pvpo* contain NP, and a few large *pvpo* cells may project to the septum and amygdala.

The ac was observed to be separated from the pv by 300-400 μm, and therefore the NP-producing cells of this magnocellular nucleus were not considered as part of the pv. No cells were found in the ac which projected to any region other than the neurohypophysis.

DISCUSSION

A differentiation of rat pv subdivisions has been noted in the present study as revealed by cell clustering and morphology, connections of projection neurons and the distribution of NP. Most significantly, neurons projecting to the neurohypophysis were found to be relatively segregated from those projecting extrahypothalamically.

Neurohypophysial-projecting neurons

Several investigators have reported the retrograde transport of HRP by magnocellular neurons of the hypothalamo-neurohypophysial system after injections into the neurohypophysis. Sherlock, Field and Raisman (1975) first observed that "lateral" pv magnocellular neurons had accumulated the enzyme, while Price and Fisher (1978) mentioned labelling in the "supero-lateral" pv. The HRP-positive cells in the "dorsolateral cap" of Ono et al. (1978) appear upon examination of their cell plots to correspond to the pvl. More recently, Hosoya and Matsushita (1979) reported pvm and pvl cell labelling following neurohypophysial HRP injections.

In the present study labelling was confined primarily to the pvm and pvl, with additional scattered cells being labelled in the dorsomedial parvocellular zone and medial to these subnuclei. The pvm appears to have gone unnoticed by most early investigators, or it simply may have been considered as part of the pvl (see Hatton et al., 1976, for discussion).

In sections reacted with DAB or H-Y and counterstained with thionine, it is obvious that the labelled neurons of the pvm and pvl have a deeply staining cytoplasm, prominent single or multiple nucleoli and a clear round or oval nucleus, the membrane of which is seldom invaginated. These same neurons respond to hormone-releasing stimuli with increases in cell size and proliferation of nucleoli (Armstrong and Hatton, 1978; Hoblitzell, Hatton and Armstrong, 1976; Hutton, 1975). Furthermore, because they are the dominant cell type in sheer numbers and density, these neurons most likely correspond to those most frequently encountered with antidromic identification techniques for the electrophysiological characterization of pv neurosecretory neurons (for reviews see Cross, Dyball, Dyer, Jones, Lincoln, Morris and Pickering, 1975; Hayward, 1977; Renaud, 1978). Thus, it is clear when considering the NP and HRP results that the magnocellular neurons of the pvm and pvl make up the classical pv neurosecretory neurons of Bargmann and co-workers (Bargmann, 1966).

Most neurons of the pvl undergo chromatolysis following neurohypophysectomy, while cells in the pvpo and parvocellular pv do not (Bodian and Maren, 1951; see "principal" portion of the pv in their Figure 5). This retrograde cell reaction in the pvl further supports the contention that most neurons in this subnucleus do not send a collateral axon outside the pituitary, as intact branches might be expected to maintain the parent somata (although see Jones, 1975, for exceptions to this generalization).

The combined results of the HRP injections and NP localization support Peterson's (1966) consideration of the ac as a neurosecretory nucleus based on Gomori staining. Sherlock, Field and Raisman (1975) also reported HRP-labelling of the ac following neurohypophysial

injections. These data contradict the opinion of Palkovits, Zaborsky and Ambach (1974), who did not include the ac in their list of accessory neurosecretory nuclei. The dorsal, periventricular location of the ac is an obvious reason for mistaking this nucleus as part of the pv. However, there is a clear rostrocaudal separation of the ac and pv. It remains to be determined whether any important functional differences further distinguish the two nuclei. Preliminary observations suggest that the ac contains mostly OX-producing cells, as does the adjacent magnocellular periventricular cell group (McNeill and Armstrong, unpublished observations).

Several authors have commented on the uneven distribution of OX and VP in the rat pv. Swaab, Pool and Nijveldt (1975) and Choy and Watkins (1977) counted a greater percentage of OX cells rostrally and VP cells caudally in the pv. This may indicate a greater proportion of OX-containing cells lie within the pvm and more VP cells are in the pvl, assuming these authors included both divisions in their counts. Indeed, preliminary observations of NP-stained material in a Brattleboro rat, which lacks the ability to synthesize VP, indicate the cell-dense core of the pvl consists of primarily VP-containing neurons, i.e., it lacks staining (McNeill and Armstrong, unpublished observations). Vandesande and Dierickx (1975) found OX cells more prevalent along the periphery of the pv, with VP cells located centrally. Unfortunately, with the absence of detailed plots or several photomicrographs in this article, no further comments can be made on the relation of this result to cell types in the pvl and pvm.

Cells lying above and dorsolateral to the fornix were also described by Sherlock, Field and Raisman (1975) to retrogradely transport HRP after neurohypophysial injections. These accessory

cells were identified by Peterson (1966) as the anterior and posterior fornical neurosecretory nuclei, and by Palkovits, Zaborsky and Ambach (1974) as accessory group III. As noted by the latter authors, the fornical nuclei have most often been termed the paraventricular accessory nuclei (e.g., Bandaranayake, 1971) and were called the lateral pv (not to be confused with the pvl) by Bodian and Maren (1951). An accessory group probably representing at least part of this complex was shown to stain for VP but not OX in the rat (see Figure 1 in Buijs et al., 1978). The posterior aspect of this accessory group will be considered again as it relates to brainstem/spinal cord projecting perikarya.

Neurons of the ac, pvm, and pvl are morphologically distinguishable from one another but exhibit many similarities. When viewing HRP-filled and Golgi-like profiles (Armstrong et al., 1979), it can be seen that cells of these areas have few dendrites which in a majority of cases project medially toward the ventricular wall. Medially directed dendrites issuing from magnocellular pv neurons have been observed in several species and these processes may encroach upon the ependymal wall (Barry, 1975; Krieg, 19732; Leontovich, 1969-70; Van den Pol, 1978). Medial dendrites may serve as receptors of CSF-borne information as has been implied for the homologous magnocellular preoptic area in lower vertebrates (Vigh and Vigh-Teichmann, 1973), they may possibly secrete hormone into the CSF (Dogterom, Van Wimersma Greidanus and Swaab, 1977), or they may simply have preferential access to the predominantly medial distribution of catecholaminergic fibers innervating the pv (McNeill and Sladek, 1978).

A paraventricular nucleus to the arcuate-external layer of the median eminence connection?

Knife cuts immediately behind the pv or lesions of this nucleus in the rat result in the removal of Gomori-positive (Bock and Jurna, 1977) and immunoreactive VP granules in the MEex (Vandesande, Dierickx and De Mey, 1977). The VP in the MEex is thought to participate in the control of ACTH release (for review, see Defendini and Zimmerman, 1978, and Zimmerman, 1976). In the present study, when HRP was given access to the arcuate-MEex region in addition to the neurohypophysis, labelling of medial parvocellular neurons was evident. Similar results were reported following tail vein injections of HRP into mice (Broadwell and Brightman, 1976). However, these small cells may not correspond to the VP-containing cells innervating the MEex.

Bodian and Maren (1951) reported an increase in the number of pv magnocellular neurons which were chromatolytic with increasing damage to the adenohypophysis. Damage to the neurohypophysis was similar in the rats with differential destruction of the adenohypophysis. This led the authors to speculate a functional relationship between the hormones of the adenohypophysis (which are regulated through hormones of the MEex) and cells of the pv. Additionally, NP-positive cells of the parvocellular variety are not commonly observed in the pv, although at least one other author has reported this phenomenon (Wolf, 1976). Thus, there remains to be demonstrated a differentiation of magnocellular and parvocellular contributions to this connection.

Using antidromic identification techniques, Pittman, Blume and Renaud (1978) discovered a few pv cells that projected to *both* the MEex and the neurohypophysis, and a considerable number that independently innervated these structures. Neurons with a firing pattern

characteristic of neurohypophysial-projecting, VP-releasing cells have been found to project to the MEex (Blume, Pittman and Renaud, 1978). Since parvocellular neurons have not been found to project to the neurohypophysis, these data suggest a magnocellular origin for the pv VP-containing connection with the MEex. At least one hormone (TRH) commonly associated with the MEex and adenohypophysial function has been localized in some medial parvocellular pv neurons (Brownfield, personal communication) and these cells have been labelled in the present study.

Brainstem/spinal cord-projecting neurons

Kuypers and Maisky (1975) first reported a projection from the dorsomedial aspect of the hypothalamus to the spinal cord in cats. Subsequently, pv neurons projecting to the lower brainstem (Saper et al., 1976) and spinal cord (Hancock, 1976; Hopkins, 1975; Ono et al., 1978; Saper et al., 1976) were identified in rat and monkey also. The results of the present study are in general agreement with these reports, but it would appear the TMB protocol afforded a greater amount of cell labelling than reported earlier with DAB.

Projections from NP-positive fibers to most autonomic nuclei of the brainstem have been observed (Swanson, 1977). The dorsal motor nucleus of the vagus and the nucleus of the solitary tract appear to receive the densest innervation (Sofroniew and Weindl, 1978a; Swanson, 1977). In the present study the attempt was made to grossly separate neurohypophysial-projecting cells from those projecting to the lower medulla and spinal cord. It is quite possible that pv neurons innervating more rostral pontine and midbrain structures (Buijs, 1978; Buijs et al., 1978; Cederbaum and Aghajanian, 1978; Saper et al.,

1976; Swanson, 1977) may be an entirely different population than those connecting with the lower brainstem/spinal cord.

Within the spinal cord the pv axons terminate primarily in the intermediolateral cell column (Saper et al., 1976; Swanson, 1977) and substantia gelatinosa (Buijs, 1978). It is possible that the pv participates in feedback control of the autonomic nervous system and modulates sensory afferent (pain?) input, respectively, via these connections. In the present study it was not possible to discern a difference in the population of pv cells projecting to the brainstem and spinal cord.

Hancock (1976) first noticed the separation of the pvpo from the pvm and pvl, and reported the former to contain the largest concentration of labelled pv neurons subsequent to spinal cord HRP injections. The relative segregation of spinal- and neurohypophysial-projecting pv neurons was first described by Ono et al. (1978). However, the latter authors reported labelling only in the dorsomedial cap, which in the present material obviously accounts for less than half the pv neurons found to project caudally. The localization of NP in cells of the pvpo and dorsomedial cap suggest that these areas are most likely responsible for the pv's predominantly oxytocinergic innervation of the brainstem and spinal cord (Buijs, 1978; Nilaver, Wilkins, Michaels, Hoffman, Silverman and Zimmerman, 1978; Swanson, 1978). It is noteworthy that although Swaab, Pool and Nijveldt (1975) found a trend toward decreasing numbers of OX-containing neurons caudally in the pv, a second, smaller peak in the numbers of these cells was detected in the extreme posterior portion of the nucleus. In the Brattleboro rat NP-positive perikarya are clustered in the ventromedial area near the pvl and scattered in the pvpo and

dorsomedial cap (McNeill and Armstrong, unpublished observations). It could be that individual OX-containing neurons in the ventromedial area of "overlap" innervate both the neurohypophysis and brainstem/spinal cord.

Hosoya and Matsushita (1979) have stressed the independence of neurohypophysial- and spinal cord-projecting neurons. Following HRP injections into the spinal cord, labelled pv cells were found *not* to contain large (2000 nm) dense cored vesicles and did not morphologically respond to water deprivation as did unlabelled magnocellular neurons. These authors concluded that the descending pv pathway does not arise from magnocellular peptide-containing cells. However, the dense concentration in the pvpo and dorsomedial cap of cells which retrogradely transport HRP from caudal injections, the substantial number of NP-positive cells in these subnuclei and the documentation of descending extrahypothalamic NP pathways suggest that much of the pv projection to the brainstem/spinal cord must be peptidergic. Thus, the intracellular distribution of NP in cells contributing to extrahypthalamic pathways may be substantially different than in cells innervating the neurohypophysis. Preliminary observations with the electron microscope have included the positive identification of large pvpo cells with but a few dense cored granules, but which contain HRP reaction product following brainstem injections (Tweedle, Hatton, Salm and Armstrong, unpublished observations). In agreement with Hosoya and Matsushita (1979), most pv cells labelled by these injections do not contain large dense cored vesicles and appear morphologically disparate from unlabelled magnocellular neurons.

A salient feature in the distribution of marked cells following caudal injections was the bridge of perikarya which stretched from

the pvpo across the dorsomedial hypothalamic nucleus and fornix to join a cluster of cells dorsal and lateral to the fornix (see Figure 8III F). This suggests an anatomical continuity among pv, postero-lateral and perifornical hypothalamic neurons which project to the brainstem and spinal cord. Caudally, the cluster of cells dorsolateral to the fornix expands into a scattered array of cells spreading to the medial edge of the cerebral peduncle. A further string of labelled cells extends laterally beneath the peduncle toward the central nucleus of the amygdala, which is also heavily labelled following brainstem, but not spinal cord, injections (also see Hopkins, 1975). This scant link of neurons between the central nucleus and the pv may in fact be but a small aspect of communion reflecting a more profound relationship between these two structures. Not only do both nuclei project to brainstem autonomic nuclei as demonstrated with autoradiographic techniques (Conrad and Pfaff, 1976; Saper et al., 1976, pv; Hopkins and Holstege, 1978, central nucleus), but both nuclei receive visceral afferent projections from the posterior aspect of the nucleus of solitary tract (Ricardo and Koh, 1978) and the parabrachial complex (Norgren, 1976; Saper and Loewy, 1978). Also, Zimmerman has found both structures to contain neurotensin-positive cells (Hatton, personal communication). These connections and the known involvement of neurotensin in temperature regulation (Bissette, Manberg, Nemeroff and Prange, 1978) implicate both the pv and central nucleus of the amygdala in the central control of autonomic function.

The difference in the number of processes arising from magno-cellular brainstem/spinal cord-projecting cells and those innervating the neurohypophysis was previously noted by Ono et al. (1978). This

difference has also been observed when viewing Golgi-like profiles of pv cells (Armstrong et al., 1979). Specifically, pvpo cells have on the average more processes than do pvm, pvl or ac neurons, and pvpo cell processes are longer and branch more frequently than those of cells in the latter subnuclei. This difference may reflect a difference in the inputs to these two basic groups of cells.

The triangular depiction of the pv and the morphology of many of his drawn cells leads one to suspect that Krieg (1932) stained primarily pvpo neurons with the Golgi method in the rat and considered them a part of his "nucleus filiformis magnocellularis." Cells in the pvpo which were densely filled with HRP in the present study were often observed to possess a long apical process which extended out toward the top of the fornix. Similar laterally extending processes have been observed in silver-impregnated neurons (Armstrong et al., 1979). Krieg (1932) described these lateral processes as initially thick extensions of the fusiform somata which gradually tapered into axons that entered the thalamic reticular nucleus or cerebral peduncle. Though he was unable to determine their targets, Krieg speculated that some of these axons turned caudally toward the midbrain. The NP-positive fibers observed in the present study which emanated from the pvpo could sometimes be seen entering the cerebral peduncle, while other fibers were seen coursing along the lateral and medial edges of this massive fiber tract. Still other fibers appeared to turn caudally, joining the medial forebrain bundle as also described by Swanson (1977). Thick, laterally extending processes of the pvpo may thus form the initial portions of axons, or axons may branch from these processes.

Projections to the amygdala and septum

Following the injection of tritiated amino acids into the pv and immediately adjacent areas, labelled fibers were seen to innervate the lateral septum and anterior and medial amygdalar nuclei in addition to other structures, including the median eminence (Conrad and Pfaff, 1976). Some of this innervation may derive from NP-producing cells, as several investigators have commented on the presence of neurophysinergic and OX- or VP-producing fibers in these areas. Swanson (1977) observed laterally extending NP-positive fibers coursing over the supraoptic nucleus to enter the medial nucleus of the amygdala. Although finding a projection to the amygdala, Sofroniew and Weindl (1978a) concluded that NP-positive fibers entered the stria terminalis to innervate the central nucleus, but did not comment on their origin. On the other hand, Buijs (1978) reported OX- and VP-positive fibers joining the stria terminalis and innervating *all* the nuclei of the amygdala, although this projection was relatively light. Buijs (1978) concluded that these fibers came from the pv.

The lateral septal nucleus receives a denser vasopressinergic innervation than does the medial area (Buijs, 1978). Conrad and Pfaff (1976) reported no labelling from pv amino acid injections in any other septal nucleus but the lateral. Apparently the VP-containing fibers in the lateral septum are finer than those usually associated with the magnocellular system. Sofroniew and Weindl (1978b) have asserted that these fine fibers originate from the VP-containing neurons of the suprachiasmatic nucleus. In the present study no suprachiasmatic neurons were labelled following septal HRP injections, and a study of the efferent projections of this nucleus revealed no such projection (Swanson and Cowan, 1975).

The present study indicates that while a few magnocellular neurons may project to the septum and amygdala, the parvocellular contingent is more substantial. However, even the labelling of small cells was not a consistent finding in amygdala-injected animals. It may be that only a few hormone-containing cells are responsible for the peptidergic innervation of these structures. Alternatively, if the projection is derived from collaterals of axons also projecting to other areas, perhaps there may be some difficulty for such fibers to accumulate enough HRP to produce visible labelling. Buijs (1978) has suggested that bi- and multipolar pv cells send processes to extrahypothalamic structures as well as to the neurohypophysis. The present results do support a small but perhaps significant projection from the pv to both the septum and amygdala which includes the labelling of a few cells which lie within the pvl and pvm, both of which are dense with neurons projecting to the neurohypophysis.

It is clear from the HRP results that efferent pv trajectories observed following tritiated amino acid injections (Conrad and Pfaff, 1976) would in all probability arise in part from adjacent neurons which are consistently labelled following HRP injections into the amygdala and particularly into the septum. Since in the study by Conrad and Pfaff the pv injection sites spread into surrounding structures, the relative contribution of the pv cannot accurately be evaluated.

General comments

The uptake of HRP by parvocellular neurons after many of the injections indicates that these pv cells must be considered as candidates for projection neurons. Krieg (1932) first found rat

parvocellular pv axons joining periventricular fibers. Axons from small pv cells have also been described as entering the lateral hypothalamus or subthalamus in mice (Barry, 1975). Golgi studies also suggest that some parvocellular neurons are intrinsic cells, i.e., with axons which do not leave pv boundaries (Barry, 1975).

The function of extrahypothalamic OX-, VP- and NP-containing pathways is not yet known, but several possibilities have been explored. Vasopressin has been implicated in avoidance learning, as its ventricular administration facilitates acquisition of, and prolongs, avoidance responding in rats normally unable to synthesize this hormone (de Wied, 1977). Furthermore, intraventricularly administered VP increases water permeability in brain tissue, and this effect is unassociated with changes in cerebral blood flow (Raichle and Grubb, 1978). Effects of this type may be related to extrahypothalamic VP.

It may be that OX, VP and the neurophysins are utilized as neurotransmitters. Ionotophoretically administered VP modulates the activity of invertebrate neurosecretory neurons (Barker and Gainer, 1974) and inhibits supraoptic neuronal activity (Nicoll and Barker, 1971). Sterba et al. (1979) have shown putative peptidergic synapses in the dorsal column nuclei and the nucleus of the solitary tract in rats and pigeons, and they conclude these originate from the magnocellular neurosecretory system. However, precise immunohistochemical procedures were not employed in that study, so the nature of these synapses is still under question. Nevertheless, their data support the contention that extrahypothalamic VP or OX may discretely interact with target neurons.

The combined results of the present investigation reveal a heterogeneous cell population in the rat pv. This is not to say that the complexity of the pv has not been appreciated previously. The pattern of labelled estrogen uptake delineates pv subdivisions (Stumpf, Sar and Keefer, 1975), although these subdivisions are not easily related to those described herein. In addition, the results of Golgi studies by Barry (1975) indicate at least four cell types may be present in the mouse pv.

It is evident that the simple "magnocellular and parvocellular" classifications of Gurdjian (1927) and Krieg (1932) can no longer be considered to adequately characterize differing pv cell types. Furthermore, the relative segregation of the neurohypophysial-projecting neurons from pv cells projecting extrahypothalamically (and particularly to the brainstem and spinal cord) suggests that the latter may operate independently from the former.

APPENDICES

APPENDIX A

EQUIPMENT AND MATERIALS

(Date of price listed in parentheses)

Horseradish peroxidase injections

1. Rat sterotaxic; David Kopf Instruments, $600.00 (1978)
2. Carrier mounted microinjection unit; David Kopf Instruments, $130.00 (1978)
3. Hypophysectomy rat ear bars; David Kopf Instruments, $250.00 (1978)
4. Hamilton 5 µl syringe with 31 gauge needle, 2" long, drawn to a 0.01" outside diameter; Anspec Co., $18.00 (1979)
5. Horseradish peroxidase (Sigma VI - $9.00/10 mg; Miles - $14.00/10 mg)
6. 1 cc tuberculin syringe with 26 gauge needle; Scientific Projects, $10.32/100 (1978)
7. Poly-l-ornithine; Sigma, $13.00/25 mg (1977)
8. Dimethylsulfoxide; Sigma, $3.50/500 ml (1977)

Histology

A. General

1. Sliding microtome, with knife; Arthur Thomas Co., $2094.00 (1978).

2. Histofreeze freezing unit; Scientific Products (no longer available)

B. Horseradish peroxidase histochemistry

1. Hanker-Yates reagent; Polysciences, $19.50/5 gm (1978-79)
2. 3,3',5,5'-tetramethylbenzidine; Sigma, $14.00/gm (1977)
3. 3,3'-diaminobenzidine; Sigma, $10.00/5 gm (1977)
4. Sodium nitro(prusside)(ferricyanide); Fisher, $55.57/lb (1977)
5. Glutaraldehyde (25%); Polysciences, $6.50/500 gm (1978-79)
6. Paraformaldehyde; Fischer, $21.66/5 lb cs (1976)
7. 2" x 3" microscope slides; Arthur Thomas Co., $9.75/ 144 (1977)
8. 48 x 60 mm cover glasses; Arthur Thomas Co., $23.22/10 oz cs (1977)
9. Thionine; Scientific Products, $35.00/25 gm (1977)
10. Neutral red; Sigma, $5.40/25 gm (1977)
11. Safranin-O; Scientific Products, $15.50/25 gm (1978)

C. Paraffin embedding, sectioning and mounting

1. Paraffin (Paraplast); Scientific Products, $2.10/2.5 lb (1977)
2. 3" x 1" microscope slides with etched end; Arthur Thomas Co., $7.40/144 (1977).
3. 24 x 60 mm cover glasses; Arthur Thomas Co., $2.85/ 1 oz box (1977)
4. Base molds (1" x 1.5" x 0.5"); Scientific Products, $30.50/ea. (1978)
5. Embedding rings; Scientific Products, $59.95/cs (1978)
6. Rotary microtome, with knife; Arthur Thomas Co., $1600.00 (1977)

Microscopy

1. Zeiss standard microscope; Morgan Instruments, $3476.00 (1977)
2. Zeiss darkfield condenser with numerical aperture of 0.6-0.75; Morgan Instruments, $227.00 (1977)
3. Microprojector (Ken-A-Vision); approx. $400.00 (1979)

Photography

1. Linhauf 5" x 7" format camera; Mark's Photoshop, approx. $1300.00 (1977)
2. Kodak contrast-process ortho film; Mark's Photoshop, $34.15/100 (1979)
3. F-5 Azo paper (8" x 10"); Mark's Photoshop, $17.30/100 (1978) Note: this paper no longer available.

APPENDIX B

HISTOLOGY

Horseradish peroxidase histochemistry

A. Using tetramethylbenzidine (TMB) or benzidine dihydrochloride (BDHC) as the chromogen. Please read section through before proceeding, as several solutions must be made in advance.

1. Perfuse rat (with descending aorta clamped) with 50-100 ml 0.89% saline followed by 200-300 ml of fixative containing 1.25% glutaraldehyde and 1% paraformaldehyde in 0.1 M phosphate buffer (pH = 7.2-7.4). If upper torso and head appear well fixed (rigid with yellowish tint), follow the fixative with 200-300 ml of cold (4°C) 0.1 M phosphate buffer with 10% sucrose added. Remove brain and place in same sucrose-buffer for 24 hr at 4°C. If rat appears poorly fixed, remove brain and soak in same fixative for 24 hr, then rinse in the 10% sucrose-buffer for 24 hr.
2. Cut sections of desired thickness into the cold sucrose-buffer solution. Sections may remain in the buffer up to 48 hr prior to reacting with good results.
3. React sections in following manner:
   a. Rinse twice, 1 min each, in distilled water.

b. Place sections for 20 min in an incubation solution which combines two solutions made independently. These are: 1) 5 mg TMB[1] in 2.5 ml 100% ETOH (heat to 40°C to dissolve TMB); and 2) 97.5 ml of solution containing 100 mg sodium nitroprusside, 92.5 ml distilled water and 5 ml of acetate buffer (made by adding 19 ml 1.0 M HCl and 61 ml distilled water). Mix solutions 1 and 2 together just prior to placing sections in. These may be made 1 hr in advance, but preferably are made fresh.

c. Add 1.5-2 ml H_2O_2 (0.3%) to solution made in "b"; react for 20 min more.

d. Place sections for 20 min into a solution prepared 2-3 hr earlier, consisting of 9 gm sodium nitroprusside, 5 ml acetate buffer (see "b"), 45 ml distilled water and 50 ml 100% ETOH. This solution should be around 0°C. I place it in the freezer prior to using it, and place in the refrigerator when in use.

e. Rinse sections twice in cold distilled water, 1 min each.

f. Mount sections immediately, or cover and place in refrigerator for a *few* hours if necessary before mounting.

g. Dry slides overnight.

---

[1]May substitute 120 mg BDHC for TMB.

h. Counterstain in 0.1% Safranin-O (or 1% Neutral red) in distilled water. The dried sections may be placed directly into the stain. Neutral red is dissolved in distilled water also, but with 40 ml acetate buffer added to each 1000 ml of water. Buffer is made by adding 50 ml 0.1 N acetic acid to 75 ml 0.1 N sodium acetate, pH = 4.5.

i. Rapidly dehydrate after brief (10 sec) distilled water rinse, in 70%, 95%, 2x 100% ETOH and twice in xylene. Alcohols should be 10 sec each. Xylene #1 should be 1 min, xylene #2 should be 10-15 min.

j. Coverslip with Permount.

B. Using Hanker-Yates reagent (H-Y) or diaminobenzidine (DAB) as the chromogen.

1. See A1

2. See A2

3. If intensification with $CoCl_2$ is desired (and it is!), then rinse sections once for 1 min in 0.1 M phosphate buffer. Then place in a filtered, 5% $CoCl_2$ solution in 0.1 M phosphate buffer, for 10 min. Rinse twice in the same buffer, 5 min each.

4. React sections in following manner:

a. Place in a solution containing 150 mg H-Y in 100 ml of phosphate buffer, with 1 ml of 1% H_2O_2 added, for 15 min. or:

for DAB, place sections in a solution containing 30 mg DAB in the same buffer for 20 min. Then add 4 ml 0.06% H_2O_2, and react for another 20 min. Reactions

with H-Y and DAB are facilitated in darkness. Both may be done at room temperature.

b. Rinse sections twice in 0.1 M phosphate buffer, 5 min each.

c. Mount sections from the same buffer, dipping each section into distilled water before placing it on the slide. This insures adhesion of the section.

d. Dry sections overnight, in oven or in air.

e. Place dried sections in xylene for 10-15 min, hydrate to distilled water (5 min in each of 100%, 95% and 70% ETOH). Keep in water 5-10 min before staining.

f. Counterstain for 20 sec in 1% thionine, made by adding 5 gm thionine to 300 ml distilled water, 113 ml 0.2 M acetic acid and 87 ml 0.2 M sodium acetate, pH = 4.5.

g. Rinse sections for 1 min in distilled water.

h. Place in 70% ETOH for 30 sec, then differentiate in 95% ETOH (with a drop of glacial acetic acid) - this may take up to a few hours or it may be done within one hour.

i. Place sections in two changes of 100% ETOH and two changes of xylene, 10 min each.

j. Coverslip with Permount.

Paraffin embedding (for immunohistochemistry)

1. Perfuse rat (with descending aorta clamped) with 50-100 ml 0.89% saline followed by 200-300 ml Bouin's fixative (made by adding 75 ml saturated picric acid to each 25 ml of 37% formaldehyde and 5 ml of glacial acetic acid).

2. Remove brain and post-fix in Bouin's for 3-4 days.

3. Embed in paraffin according to following schedule:

   a. Wash overnight in running tap water (place cheesecloth over mouth of jar with the brain inside).

   b. Block the brain if desired.

   c. Dehydrate:

	30% ETOH	overnight
	50% ETOH	2 hr
	70% ETOH	2 hr
	95% ETOH	2 hr
	100% ETOH	1 hr
fresh	100% ETOH	1 hr
	methyl benzoate + 100% ETOH (equal volumes)	1 hr
used	methyl benzoate	1 hr
fresh	methyl benzoate	1 hr

   d. In oven at 60°C

fresh paraffin	1 hr
fresh paraffin	1 hr
fresh paraffin	1 hr
fresh paraffin	1 hr

   embed in fresh paraffin

   e. To embed, pour small amount of paraffin in greased (use vaseline or silicone) metal base mold.

   f. When firm (but not hard!), place brain on the layer of paraffin.

   g. Place embedding ring on top of base mold, and fill mold with paraffin.

h. Allow paraffin to harden overnight.

i. Remove paraffin block from mold, pare edges down to a rectangle containing the brain and section block at 6-10 μm on a rotary microtome.

j. Mount sections from heated water (52-56°C) onto 1" x 3" slides which previously have been coated with 1% geltain and 0.3% chromium potassium sulfate and baked in the oven for an hour.

k. Dry slides vertically on slotted, wooden rack. Then dry in oven overnight.

l. Deparaffinize sections in 4 changes of xylene, 20 min each.

m. Hydrate according to following schedule:

100% ETOH	10 min
95% ETOH	10 min
70% ETOH	20 min
50% ETOH	20 min
distilled H_2O	20 min
phosphate-buffered saline (0.01 M, pH = 7.2)	20 min

n. Stain according to peroxidase-antiperoxidase method of Sternberger (1974).

o. Sections may be lightly counterstained with thionine (see B, 4, f, under HRP histochemistry) or cresyl violet.

APPENDIX C

RAW DATA

HRP positive cell counts from rat 051078

These were made from alternate sections, 60 μm in thickness, which had been reacted with TMB and counterstained with neutral red. Counts were made on the left side only, through the paraventricular nucleus.

section #	# cells	
	>14 μm	≤14 μm
1, IV, III	24	24
1, IV, IV	103	13
2, I, I	278	62
2, I, II	397	63
2, I, III	106	39
2, I, IV	18	29
2, II, I	1	0
2, II, II	2	0
	929 +	230 = 1159 total

Cells ≤14 μm account for $\frac{230}{1159}$, or 19.84% of total.

LIST OF REFERENCES

LIST OF REFERENCES

Adams, J. C. 1977. Technical considerations on the use of HRP as a neuronal marker. Neuroscience, 2: 141-146.

Armstrong, W. E., and G. I. Hatton. 1978. Morphological changes in the rat supraoptic and paraventricular nuclei during the diurnal cycle. Brain Res., 157: 407-413.

Armstrong, W. E., S. Warach, G. I. Hatton and T. H. McNeill. 1979. Subnuclei in the rat hypothalamic paraventricular nucleus: a cytoarchitectural, HRP and immunocytochemical analysis. Submitted for publication.

Bandaranayake, R. C. 1971. Morphology of the accessory neurosecretory nuclei and of the retrochiasmatic part of the supraoptic nucleus of the rat. Acta Anat., 80: 14-22.

Bargmann, W. 1966. Neurosecretion. Int. Rev. Cytol., 19: 183-201.

Bargmann, W., and E. Scharrer. 1951. The site of origin of the hormones of the posterior pituitary. Amer. Sci., 39: 255-259.

Barker, J. L., and H. Gainer. 1974. Peptide regulation of bursting pacemaker activity in a molluscan neurosecretory cell. Science, 184: 1371-1373.

Barry, J. 1975. Essai de classification, en technique de Golgi, des diverses categories de neurones du noyau paraventriculaire chez la souris. Comp. Rend. Soc. Biol., 169: 978-980.

Bissette, G., P. Manberg, C. B. Nemeroff and A. J. Prange. 1978. Neurotensin, a biologically active peptide. Life Sci., 23: 2173-2182.

Blume, H. W., Q. J. Pittman and L. P. Renaud. 1978. Electrophysiological indications of a 'vasopressinergic' innervation of the median eminence. Brain Res., 155: 153-158.

Bock, R., and I. Jurna. 1977. Ipsilateral diminution of CRF-granules after unilateral hypothalamic lesions. Cell Tiss. Res., 185: 191-198.

Bodian, D., and T. H. Maren. 1951. The effect of neuro- and adenohypophysectomy on retrograde degeneration in hypothalamic nuclei of the rat. J. Comp. Neur., 94: 485-512.

Broadwell, R. D., and M. W. Brightman. 1976. Entry of peroxidase into neurons of the central and peripheral nervous systems from extracerebral and cerebral blood. J. Comp. Neur., 166: 257-284.

Buijs, R. M. 1978. Intra- and extrahypothalamic vasopressin and oxytocin pathways in the rat. Pathways to limbic system, medulla oblongata and spinal cord. Cell Tiss. Res., 192: 423-436.

Buijs, R. M., D. F. Swaab, J. Dogterom and F. W. Van Leeuwen. 1978. Intra- and extrahypothalamic vasopressin and oxytocin pathways in the rat. Cell Tiss. Res., 186: 423-433.

Bunt, A. H., A. E. Hendrickson, J. S. Lund, R. D. Lund and A. F. Fuchs. 1975. Monkey retinal ganglion cells: morphometric analysis and tracing of axonal projections, with a consideration of the peroxidase technique. J. Comp. Neur., 164:265-286.

Cedarbaum, J. M., and G. K. Aghajanian. 1978. Afferent projections to the rat locus coeruleus as determined by a retrograde tracing technique. J. Comp. Neur., 178: 1-16.

Cheng, K. W., and H. G. Friesen. 1971. A radioimmunoassay for vasopressin binding proteins - neurophysin. Endocrinology, 88: 608-619.

Choy, V. J., and W. B. Watkins. 1977. Immunocytochemical study of the hypothalamo-neurohypophysial system. II. Distribution of neurophysin, vasopressin and oxytocin in the normal and osmotically stimulated rat. Cell Tiss. Res., 180: 467-490.

Christ, J. F. 1966. Nerve supply, blood supply and cytology of the neurohypophysis. In *The Pituitary Gland*, Vol. 3. G. W. Harris and B. T. Donovan, eds. University of California Press, Berkeley, pp. 62-130.

Christ, J. F. 1969. Derivation and boundaries of the hypothalamus, with atlas of hypothalamic grisea. In *The Hypothalamus*. W. Haymaker, E. Anderson and W. J. H. Nauta, eds. Charles C. Thomas, Springfield, IL, pp. 13-60.

Conrad, L. C. A., and D. W. Pfaff. 1976. Efferents from medial basal forebrain and hypothalamus in the rat. II. An autoradiographic study of the anterior hypothalamus. J. Comp. Neur., 169: 221-262.

Cross, B. A., R. E. J. Dyball, R. G. Dyer, C. W. Jones, D. W. Lincoln, J. F. Morris and B. T. Pickering. 1975. Endocrine neurones. Rec. Prog. Horm. Res., 31: 243-294.

Defendini, R., and E. A. Zimmerman. 1978. The magnocellular neurosecretory system of the mammalian hypothalamus. In *The Hypothalamus*. S. Reichlin, R. J. Baldessarini and J. B. Martin, eds. Raven Press, New York, pp. 137-152.

Dogterom, J., F. G. M. Snijdewint and R. M. Buijs. 1978. The distribution of vasopressin and oxytocin in the rat brain. Neurosci. Letters, 9: 341-346.

Dogterom, J., Tj. B. Vanwimersma Greidanus and D. F. Swaab. 1977. Evidence for the release of vasopressin and oxytocin into cerebrospinal fluid: measurements in plasma and CSF of intact and hypophysectomized rats. Neuroendocrinology, 24: 108-118.

Gurdjian, E. S. 1927. The diencephalon of the albino rat. Studies on the brain of the rat. No. 2. J. Comp. Neur., 43: 1-114.

Hadley, R. T., and M. C. Trachtenberg. 1978. Poly-L-ornithine enhances the uptake of horseradish peroxidase. Brain Res., 158: 1-14.

Halperin, J. J., and J. H. Lavail. 1975. A study of the dynamics of retrograde transport of horseradish peroxidase in injured neurons. Brain Res., 100: 253-270.

Hancock, M. B. 1976. Cells of origin of hypothalamo-spinal projections in the rat. Neurosci. Letters, 3: 179-184.

Hanker, J. S., P. E. Yates, C. B. Metz and A. Rustioni. 1977. A new specific, sensitive and non-carcinogenic reagent for the demonstration of horseradish peroxidase. Histochem. J., 9: 789-792.

Hatton, G. I., U. E. Hutton, E. R. Hoblitzell and W. E. Armstrong. 1976. Morphological evidence for two populations of magnocellular elements in the rat paraventricular nucleus. Brain Res., 108: 187-193.

Hatton, G. I., and J. K. Walters. 1973. Induced multiple nucleoli, nucleolar margination, and cell size changes in supraoptic neurons during dehydration and rehydration in the rat. Brain Res., 59: 137-154.

Hayward, J. N. 1977. Functional and morphological aspects of hypothalamic neurons. Physiol. Rev., 57: 574-658.

Herkenham, M., and W. J. H. Nauta. 1977. Afferent connections of the habenular nuclei in the rat. A horseradish peroxidase study, with a note on the fiber-of-passage problem. J. Comp. Neur., 173: 123-146.

Hoblitzell, R. R., G. I. Hatton and W. E. Armstrong. 1976. Paraventricular nucleus: changes in the medial and lateral cell groups during dehydration and rehydration in the rat. Brain Res. Bull., 1: 329-332.

Hopkins, D. A. 1975. Amygdalotegmental projections in the rat, cat and rhesus monkey. Neurosci. Letters, 1: 263-270.

Hopkins, D. A. and G. Holstege. 1978. Amygdaloid projections to the mesencephalon, pons and medulla oblongata in the cat. Exp. Brain Res., 32: 529-548.

Hosoya, Y., and M. Matsushita. 1979. Identification and distribution of the spinal and hypophysial projection neurons in the paraventricular nucleus of the rat: a light and electron microscopic study with the horseradish peroxidase method. Exp. Brain Res., 35: 315-332.

Hutton, U. E. 1975. Changes in the paraventricular nucleus during different stages of pregnancy and lactation in the albino rat. Unpublished Master's Thesis, Michigan State University.

Itaya, S. K., T. H. Williams and E. L. Engel. 1978. Anterograde transport of horseradish peroxidase enhanced by poly-l-ornithine. Brain Res., 150: 170-176.

Jones, E. G. 1975. Possible determinants of the degree of retrograde neuronal labeling with horseradish peroxidase. Brain Res., 85: 249-254.

Keefer, D. A. 1978. Horseradish peroxidase as a retrogradely-transported dendritic marker. Brain Res., 140: 15-32.

Krieg, W. J. S. 1932. The hypothalamus of the albino rat. J. Comp. Neur., 55: 19-89.

Kuypers, H. G. J. M., and V. A. Maisky. 1975. Retrograde axonal transport of horseradish peroxidase from spinal cord to brainstem cell groups in the cat. Neurosci. Letters, 1: 9-14.

Leontovich, T. A. 1969-70. The neurons of the magnocellular neurosecretory nuclei of the dog's hypothalamus. A Golgi study. J. Hirnfor., 11: 499-517.

McNeill, T. H., and J. R. Sladek, Jr. 1978. Comparative catecholamine-neurophysin morphology in the rat supraoptic and paraventricular nuclei. Soc. Neurosci. Abstr., 4: 279.

Mesulam, M.-M. 1976. The blue reaction product in horseradish peroxidase neurohistochemistry: incubation parameters and visibility. J. Histochem. Cytochem., 24: 1273-1280.

Mesulam, M.-M. 1978. Tetramethylbenzidine for horseradish neurochemistry: a non-carcinogenic blue reaction-product with superior sensitivity for visualizing afferents and efferents. J. Histochem. Cytochem., 26: 106-117.

Nauta, H. J. W., M. B. Pritz and R. J. Lasek. 1974. Afferents to the rat caudo-putamen studied with horseradish peroxidase. An evaluation of a retrograde neuroanatomical research method. Brain Res., 67: 219-238.

Nicoll, R. A., and J. L. Barker 1971. The pharmacology of recurrent inhibition in the supraoptic neurosecretory system. Brain Res., 35: 501-511.

Nilaver, G., J. Wilkins, J. Michaels, D. L. Hoffman, A. J. Silverman and E. A. Zimmerman. 1978. Oxytocin-neurophysin pathways to the lower brainstem and spinal cord of the rat. Soc. Neurosci. Abstr., 4: 1118.

Norgren, R. 1976. Taste pathways to hypothalamus and amygdala. J. Comp. Neur., 166: 17-30.

Ono, T., H. Nishino, K. Sasaka, K. Muramoto, I. Yano and A. Simpson. 1978. Paraventricular nucleus connections to spinal cord and pituitary. Neurosci. Letters, 10: 141-146.

Palkovits, M., L. Zaborsky and G. Ambach. 1974. Accessory neurosecretory cell groups in the rat hypothalamus. Acta Morphol. Acad. Sci. Hung., 22(1): 21-33.

Peterson, R. P. 1966. Magnocellular neurosecretory centers in the rat hypothalamus. J. Comp. Neur., 128: 181-190.

Pittman, Q. J., H. W. Blume and L. P. Renaud. 1978. Electrophysiological indications that individual hypothalamic neurons innervate both median eminence and neurohypophysis. Brain Res., 157: 364-368.

Poulain, D. A., J. B. Wakerley and R. E. J. Dyball. 1977. Electrophysiological differentiation of oxytocin- and vasopressin-secreting neurons. Proc. Roy. Soc. Lond., 196: 367-384.

Price, P., and A. W. F. Fisher. 1978. Electron microscopical study of retrograde axonal transport of horseradish peroxidase in the supraoptico hypophyseal tract in the rat. J. Anat., 125: 137-148.

Raichle, M. E., and R. L. Grubb, Jr. 1978. Regulation of brain water permeability by centrally-released vasopressin. Brain Res., 143: 191-194.

Renaud, L. P. 1978. Neurophysiological organization of the endocrine hypothalamus. In *The Hypothalamus*. S. Reichlin, R. J. Baldessarini and J. B. Martin, eds. Raven Press, New York, pp. 269-302.

Ricardo, J. A., and E. T. Koh. 1978. Anatomical evidence of direct projections from the nucleus of the solitary tract to the hypothalamus, amygdala and other forebrain structures in the rat. Brain Res., 153: 1-26.

Richard, Ph., M. J. Freund-Mercier and F. Moos. 1978. Hypothalamic neurones with an endocrine function. Identification, localization, electrophysiological characteristics and hormonal control. J. Physiol. (Paris), 74: 61-112.

Robinson, A. G., E. A. Zimmerman, E. G. Engleman, and A. G. Frantz. 1971. Radioimmunoassay of bovine neurophysin: specificity of neurophysin I and neurophysin II. Metabolism, 20: 1138-1147.

Saper, C. B., and A. D. Loewy. 1978. Efferent projections of the parabrachial nucleus. Soc. Neurosci. Abstr., 4: 24.

Saper, C. B., A. D. Loewy, L. W. Swanson and W. M. Cowan. 1976. Direct hypothalamo-autonomic connections. Brain Res., 117: 305-312.

Seif, S. M., A. B. Huellmantel, M. P. Platia, C. Haluszczak and A. G. Robinson. 1971. Isolation, radioimmunoassay and physiologic secretion of rat neurophysins. Endocrinology, 100: 1317-1326.

Sherlock, D. A., P. M. Field and G. A. Raisman. 1975. Retrograde transport of horseradish peroxidase in the magnocellular neurosecretory system of the rat. Brain Res., 88: 403-414.

Silverman, A. J., and E. A. Zimmerman. 1975. Ultrastructural immunocytochemical localization of neurophysin and vasopressin in the median eminence and posterior pituitary of guinea pig. Cell Tiss. Res., 159: 291-301.

Sofroniew, M. V., and A. Weindl. 1978a. Extrahypothalamic neurophysin-containing perikarya, fiber pathways and fiber clusters in rat brain. Endocrinology, 102: 334-337.

Sofroniew, M. V., and A. Weindl. 1978b. Projections from the parvocellular vasopressin- and neurophysin-containing neurons of the suprachiasmatic nucleus. Amer. J. Anat., 153: 391-430.

Sterba, G., G. Hoheisel, R. Wegelin, W. Naumann and F. Schober. 1979. Peptide containing vesicles within neuro-neuronal synapses. Brain Res., 169: 55-64.

Sternberger, L. A. 1974. *Immunocytochemistry*. Prentice-Hall, Inc., Englewood Cliffs, NJ.

Stumpf, W. E., M. Sar and D. A. Keefer. 1975. Atlas of estrogen target cells in rat brain. In *Anatomical Endocrinology*. W. E. Stumpf and L. D. Grant, eds. Karger, Basel, pp. 104-119.

Swaab, D. F., C. W. Pool and F. Nijveldt. 1975. Immunofluorescence of vasopressin and oxytocin in the rat hypothalamo-neurohypophysial system. J. Neural Trans., 36: 195-216.

Swanson, L. W. 1977. Immunohistochemical evidence for a neurophysin-containing autonomic pathway arising in the paraventricular nucleus of the hypothalamus. Brain Res., 128: 346-353.

Swanson, L. W. 1978. Extra-hypophysial oxytocin-containing pathways in the brain and spinal cord of the rat and monkey. Soc. Neurosci. Abstr., 4: 415.

Swanson, L. W., and W. M. Cowan. 1975. The efferent connections of the suprachiasmatic nucleus of the hypothalamus. J. Comp. Neur., 160: 1-12.

Van den Pol, A. N. 1978. A Golgi and EM study of the rat hypothalamic magnocellular paraventricular nucleus. Soc. Neurosci. Abstr., 4: 357.

Vandesande, F., and K. Dierickx. 1975. Identification of the vasopressin producing and of the oxytocin producing neurons in the hypothalamic magnocellular neurosecretory system of the rat. Cell Tiss. Res., 165: 153-162.

Vandesande, F., K. Dierickx and J. De Mey. 1977. The origin of the vasopressinergic and oxytocinergic fibres of the external layer of the median eminence of the rat hypophysis. Cell Tiss. Res., 180: 443-452.

Vigh, B., and I. Vigh-Teichmann. 1973. Comparative ultrastructure of the cerebrospinal fluid-contacting neurons. Int. Rev. Cytol., 35: 189-252.

Wied, D. de 1977. Peptides and behavior. Life Sci., 20: 195-204.

Wolf, G. 1976. Immunohistological identification of neurophysin and neurophysin-like substances in different vertebrates. Endokrinologie, 68: 288-299.

Zimmerman, E. A. 1976. Localization of hypothalamic hormones by immunocytochemical techniques. In *Frontiers in Neuroendocrinology*, Vol. 4. L. Martini and W. Ganong, eds. Raven Press, New York, pp. 25-62.

Zimmerman, E. A., K. C. Hsu, A. G. Robinson, P. W. Carmel, A. G. Frantz and M. Tannenbaum. 1973. Studies of neurophysin secreting neurons with immunoperoxidase techniques employing antibody to bovine neurophysin. I. Light microscopic findings in monkey and bovine tissues. Endocrinology, 92: 931-940.

Zimmerman, E. A., R. Defendini, H. W. Sokol and A. G. Robinson. 1975. The distribution of neurophysin-secreting pathways in the mammalian brain. Light microscopic studies using the immunoperoxidase technique. Ann. NY Acad. Sci., 248: 92-111.

MICHIGAN STATE UNIV. LIBRARIES
31293100628779